AFOSR-TR-96

0359

REPORT DOCUMENTATION PAGE

1. AGENCY USE ONLY (Leave blank)	2. REPORT DATE	3. REPORT TYPE AND DATES COVERED
	5/1/96	FINAL REPORT - 01 May 93 - 30 Apr 96

4. TITLE AND SUBTITLE

ULTRA-HIGH SPEED COMPOUND SEMICONDUCTOR PHOTONICS

5. FUNDING NUMBERS

61102F
2305/AS

6. AUTHOR(S)

J. Peter Krusius

7. PERFORMING ORGANIZATION NAME(S) AND ADDRESS(ES)

Cornell University
406 Phillips Hall
Ithaca, NY 14853

8. PERFORMING ORGANIZATION REPORT NUMBER

9. SPONSORING / MONITORING AGENCY NAME(S) AND ADDRESS(ES)

Air Force Office of Scientific Research - NE
Maj. William W. Arrasmith
Suite B115
Bolling Air Force Base, DC 20332-0001

10. SPONSORING / MONITORING AGENCY REPORT NUMBER

F49620-93-C-0016

11. SUPPLEMENTARY NOTES

12a. DISTRIBUTION / AVAILABILITY STATEMENT

APPROVED FOR PUBLIC RELEASE.
DISTRIBUTION UNLIMITED.

12b. DISTRIBUTION CODE

13. ABSTRACT *(Maximum 200 words)*

This document is the third annual report on research conducted under the auspices of the Joint Services Electronics Program at Cornell University. The research has been organized under the integrated theme "Ultra-High Speed Compound Semiconductor Photonics." Results on OMVPE materials growth, femtosecond optical probing of thin films, quantum wells and device structures, ensemble Monte Carlo simulation of pump-and-probe thin film experiments and optoelectronic detectors, design and fabrication of strain compensated multi-quantum-well high speed vertical cavity lasers, and fabrication of integrated high speed metal-semiconductor-metal light detectors. Work has progressed according to plan. This research will continue under a new three year contract.

19960726 079

14. SUBJECT TERMS

Compound semiconductor, organometallic vapor phase epitaxy, femtosecond laser sources, femtosecond laser probing, Monte Carlo simulation of photogenerated carriers, quantum well laser, metal-semi-*

15. NUMBER OF PAGES

80

16. PRICE CODE

17. SECURITY CLASSIFICATION OF REPORT	18. SECURITY CLASSIFICATION OF THIS PAGE	19. SECURITY CLASSIFICATION OF ABSTRACT	20. LIMITATION OF ABSTRACT
UNCLASSIFIED	UNCLASSIFIED	UNCLASSIFIED	UL

...r distribu...unlimited

Final

~~ANNUAL~~ REPORT

ULTRA-HIGH SPEED COMPOUND SEMICONDUCTOR PHOTONICS

MAY 1, 1995 - APRIL 30, 1996

CONTRACT #F49620-93-C-0016

AIR FORCE ... (AFSC)
NOTICE ...
This ... ewed and is
appro... R 190-12.
distri...
Joan Bo...
STINFO Program Manager

CORNELL UNIVERSITY

SCHOOL OF ELECTRICAL ENGINEERING

ITHACA, NEW YORK 14853

Final

~~ANNUAL~~ REPORT

ULTRA-HIGH SPEED COMPOUND SEMICONDUCTOR PHOTONICS

MAY 1, 1995 - APRIL 30, 1996

CONTRACT #F49620-93-C-0016

ANNUAL REPORT

Joint Services Electronics Program
Contract #F49620-93-C-0016
May 1, 1995 - April 30, 1996

ULTRA-HIGH SPEED COMPOUND SEMICONDUCTOR PHOTONICS

May 1, 1996

J.P. Krusius
Principal Investigator

Cornell University,
School of Electrical Engineering
Ithaca, New York 14853

TABLE OF CONTENTS

A. DIRECTOR'S OVERVIEW

This document is the third and final annual report of the Cornell Joint Services Electronics Program for the period from May 1, 1993 to April 30, 1996. This report cover the time interval from May 1, 1995 to April 30, 1996. The program is focused on ultra-high speed compound semiconductor photonics with work units on compound semiconductors materials growth, femtosecond optical sources and characterization of materials and devices, device physics and simulation, device design and fabrication components in a synergistic fashion. Six task investigators, Profs. R. Shealy, C. Tang, C. Pollock, P. Krusius, Y. Lo and R. Compton, with their graduate students have contributed to JSEP research. The interactions and collaborations between the participating groups have progressed according to plan. The interactions of the two recently added device tasks, one high speed light sources and other one light detectors, with other tasks of the program have borne fruit. 7 MS/PhD graduate students and two research staff members have been partially, or fully, supported by JSEP this year. A total of 48 publications and 6 theses were written in this period and are now in various stages of processing. 6 PhD degrees have been awarded to JSEP supported students during this reporting period and several others are close to finishing.

A group of faculty with extensive expertise and track record in compound semiconductor materials, electronic devices, femtosecond optical sources and measurements methods, photonic devices, micro and nanofabrication and device physics. Indicators of this strength are, for example: past JSEP programs, which during their 16 year history have focused compound semiconductor materials and high speed electronic devices and femtosecond optics; the Optoelectronics Technology Center, a consortium consisting of Cornell University, University of California Santa Barbara, University of California San Diego, which is supported by ARPA and is in its second three year phase; the Cornell Nanofabrication Facility supported by the National Science Foundation and industry, one of the major nodes in the National Nanofabrication Network; the Materials Science Center supported by the National Science Foundation; the Cornell Center for Theory and Simulation, one of the national supercomputer centers supported by the National Science Foundation; and many individual programs supported by federal and industrial sources. The Compound Semiconductor Materials Growth Facility with several OMVPE reactors; the Optoelectronics Laboratory for optical experiments and measurements within the School of Electrical Engineering; and several unique tunable femtosecond laser sources and complete femtosecond optical characterization laboratories are unique resources for the JSEP research.

B. DESCRIPTION OF SPECIAL ACCOMPLISHMENTS AND TECHNOLOGY TRANSITION

B.1 DESCRIPTION OF SPECIAL ACCOMPLISHMENTS AND TECHNOLOGY TRANSITION

A number of significant achievements have been reached during this reporting period. The organometallic vapor phase epitaxial (OMVPE) compound semiconductor materials growth effort under the leadership of Prof. R. Shealy has focused on flow modulation epitaxial growth of InP/GaInAs pseudo-alloys, characterization of arsenide to phosphide interfaces, and fabrication of preliminary laser devices for the 1.3 μm wavelength. The shortest period superlattice built to date in the GaInAs/InP materials system have been demonstrated. These layers have been used to fabricate broad area superlattice heterostructure lasers (SL-SCH type). Threshold currents as low 3 kA/cm^2 at room temperature have been obtained in unoptimized structures. This group is hoping to improve the room temperature performance of these pseudo-alloy devices. If this can be done, these laser devices are expected to have a large impact on fiber-optic communication.

The research into new tunable femtosecond sources and their use to characterize compound semiconductor thin films via femtosecond optical probes has continued under the direction of Prof. Tang. This group has demonstrated for the first time the operation of a high power, average repetition rate femtosecond $KNbO_3$ based optical parametric oscillator (OPO) that is continuously tunable in the wavelength range from 2.3 to 5.2 μm. Pulses as short as 60 femtoseconds (fs) were measured. With this results this group has continuous spectral coverage from the visible light to 5.2 μm wavelength in the femtosecond time domain. They are working together with the Air Force Phillips Laboratory on HgCdTe materials that are transparent to 2.8 μm. The objective is to measure ultrafast relaxation times for hot electronics using the tunable femtosecond laser sources developed in Prof. Tang's group.

Pollock's research group has completed the femtosecond measurements of carrier dynamics in highly doped $In_{0.53}Ga_{0.47}As$ thin films, both n-and p-type, using near band-edge time-resolved femtosecond optical transmission correlation. With their additive pulse modelocked (APM) NaCl laser, operating with 0.8 eV pulses, they have probed the behavior of photogenerated carriers near the Fermi level. Measurements have focused on heavily doped InGaAs thin films on InP in order to explore the effect of background charge on the relaxtion of the optically generated electron-hole plasma in collaboration with Prof. Krusius' effort. Pollock's group has interacted with two Air Force Laboratories. In the first interaction with Mark Krol from Rome Laboratory Photonics Center, Griffiss Air Force Base, they are

attempting to characterize double quantum well structures prepared at Rome Laboratories. The second interaction occurs with the Phillips Laboratory, Kirtland Air Force Base on controlling chaos primarily via synchronization and control of chaotic oscillators. This work will carry into the next three year program period.

The research group of Prof. J.P. Krusius has successfully extended their dual carrier Monte Carlo formulation to MSM and PIN photodetectors. Their earlier formulation was developed for femtosecond relaxation of an optically generated electron-hole plasma under dual-pulse correlation and pump-and-probe spectroscopy conditions. This group is now in a position to study the intrinsic response of photodetectors based on a first principles approach on the pico/femtosecond time scale on a more rigorous and fundamental level than anybody before. First correlations with measured data show good overall agreement. The group is in the process of mapping out the role of various carrier process, fundamental limits, and practical ultra-high speed photodetector designs. The group has collaborated with the research group of Prof. Compton on MSM detector response correlations and designs. Efforts are under way to design the fastest response MSM detectors jointly with Prof. Compton. The Krusius' group has continued to further collaborate with Pollock's femtosecond measurement effort with the primary focus on carrier relaxation in heavily doped thin films in the InGaAs/InP system. The electron-hole plasma relaxation response on longer time scales beyond the autocorrelation width (~ 200 fs) appears now well understood, but complications on the shortest time scales remain to be resolved.

Prof. Lo's group has been working on vertical cavity surface emitting lasers (VCSEL) with strain-compensated multiple quantum wells (SC-MQW). They have worked on new SC-MQW laser structures on materials from R. Shealy and Bellcore with the goal of making VCSELs for the 1.3/1.55 μm wavelengths. They have developed a new mirror forming technique based on wafer bonding. This group has demonstrated 1.55 μm VCSELs with threshold currents of 10 -16 mA at room temperature, a results among the lowest reported to date. They also have developed an extensive theoretical framework for quantum well laser modeling, which facilitates quantitative design and analysis of the modulation response. Continuous wave operation of these laser structures is the next goal for this group. A wide range of applications awaits these lasers in parallel optical links, optical microwave links, phase array antennas, fiber sensors, fiber optic gyroscopes, and gas sensing to name some of them This group has interacted with JSEP tasks of Shealy, Pollock, and Krusius.

Prof. Compton's group has made progress on the fabrication and characterization of high speed metal-semiconductor-metal (MSM) detectors. They have successfully fabricated AlnAs/GaInAs MSM photodetectors on materials grown via molecular beam epitaxy (MBE) and metallo-organic

chemical vapor phase epitaxy (MOCVD). Cu Schottky barriers with improved characteristics to the common Ti/Pt/Au have been demonstrated. Low dark currents in the 4 $pA/\mu m^2$ and response time in the 17 ps (FWHM) range were obtained. These results are comparable to the best ones for any long wavelength MSM photodetector. This group has collaborated with the JSEP tasks of R. Shealy and P. Krusius.

Further special accomplishments are listed in the description of research under each of the tasks.

B.2 VIEWGRAPHS OF SPECIAL ACCOMPLISHMENTS AND TECHNOLOGY TRANSITION

Cornell JSEP (F49620-90-C0039) Task : J.R. Shealy
1.3 μm InP-Based Laser w/ Superlattice Gain Media

The Device Structure

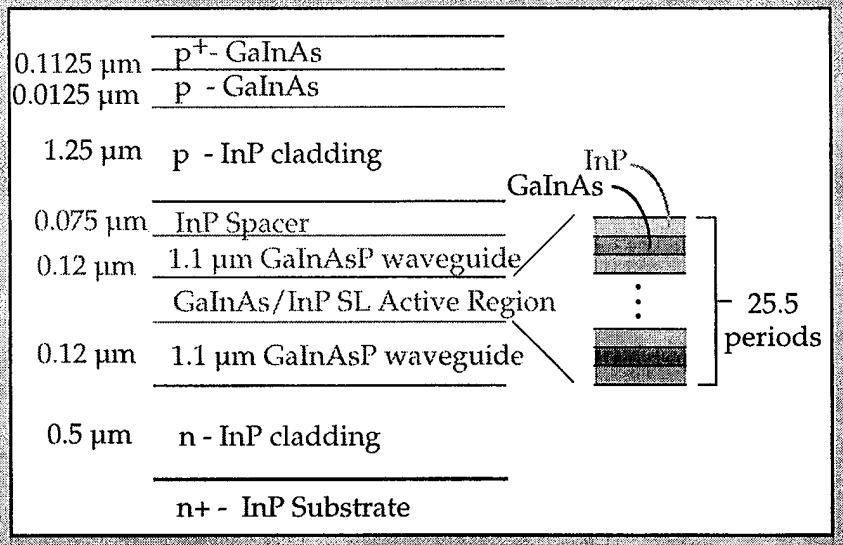

Threshold Data

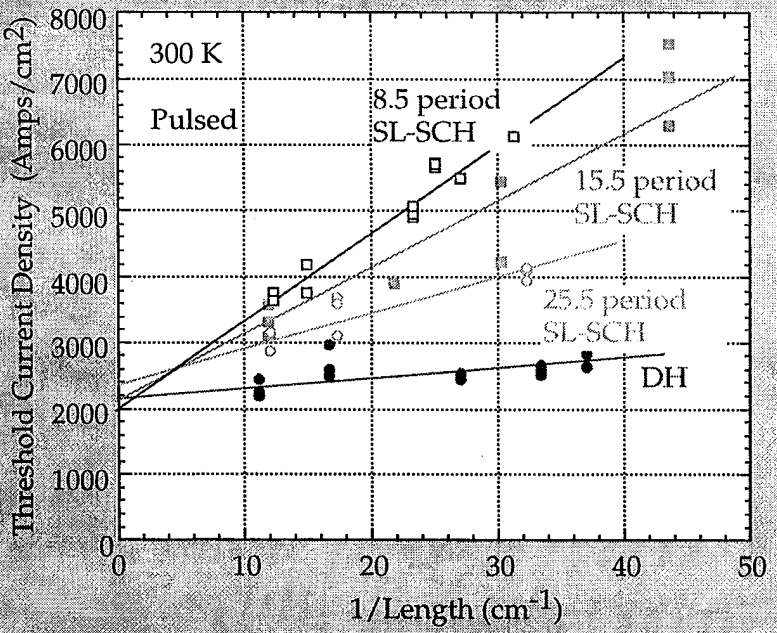

OBJECTIVE

- Demonstrate the First 1.3 μm Laser with a Pseudo-Alloy (InP/GaInAs SL) Optical Gain Media
- Examine Device Performance Characteristics with Emphasis on Improved Temperature Performance

RESULTS

- Reasonable 300 K Threshold Performance
- Simple Model Explaining the Inverse Length Data: Slope α 1/number of periods
- SL Device Performance Lies Between the Bulk and MQW Active Region Extremes

Cornell JSEP (F49620-90-C0039) Task: C. L. Tang
Femtosecond Laser Studies of Ultrafast Processes in Compound Semiconductors

Highlights :

- Developed first high average power, high-repetition rate femtosecond (fs) tunable source in the mid infrared spectral range to 5.2 μm for applications in the study of ultrafast processes in compound semiconductors.

- Relaxation studies of ultrafast hole dynamics in GaAs and hot electrons in InGaAsP and HgCdTe under study using mid-infrared fs tunable sources.

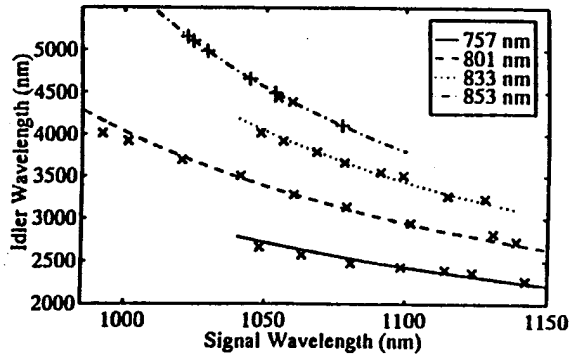

FIG. 1. Signal/idler wavelengths generated by the fs-OPO for several different pump wavelengths. (X marks represent measured signal/idler pairs; crosses denote inferred idler wavelengths from measured signal and pump wavelengths.)

Signal/idler wavelengths to 5.2 μm generated by the fs-OPO for several pump wavelengths

Publications :

- "High average power, high-repetion rate femtosecond pulse generation in the 1-5 μm region using an optical parametric oscillator", App. Phys. Lett. 68, 452(1996)

- *Fundamentals of Optical Parametric Processes and Oscillators* (Harwood Academic Press, 1996).

- "Ultrashort pulse phenomena", invited article to be published in *Encyclopedia of Applied Physics*, eds. G. L. Trigg and E. S. Vera, (VCH Publishers)

Award:

1996 Charles H. Townes Award

Cornell JSEP (F49620-90-C0039) Task: C. R. Pollock
Observation of Period-Doubling Behavior in Femtosecond Laser

Objectives:

- Develop a laser source that displays chaotic output
- To develop methods for fast chaotic control of lasers using small perturbations
- To extend chaotic control to speeds beyond 100 MHz, and to develop methods for controlling chaos in fast lasers
- Interact with USAF Phillips Lab to experimentally observe, control, and theoretically model chaos in lasers

Accomplishments:

- Observation of period doubling and quasi-periodicity up to n=4 in a Additive Pulse Modelocked color center laser
- Acquisition of long time series for analysis, model testing, and system characterization by Nonlinear Optics Division at USAF Phillips Lab
- Variation of phase between coupled cavities as a bifurcation control parameter

Approach:

- Achieve a predictable route for bifurcations of the period doubling (system characterization)
- Use continuous phase delayed feedback to control period orbits of the laser
- Attempt other control techniques such as intracavity phase and gain modulation

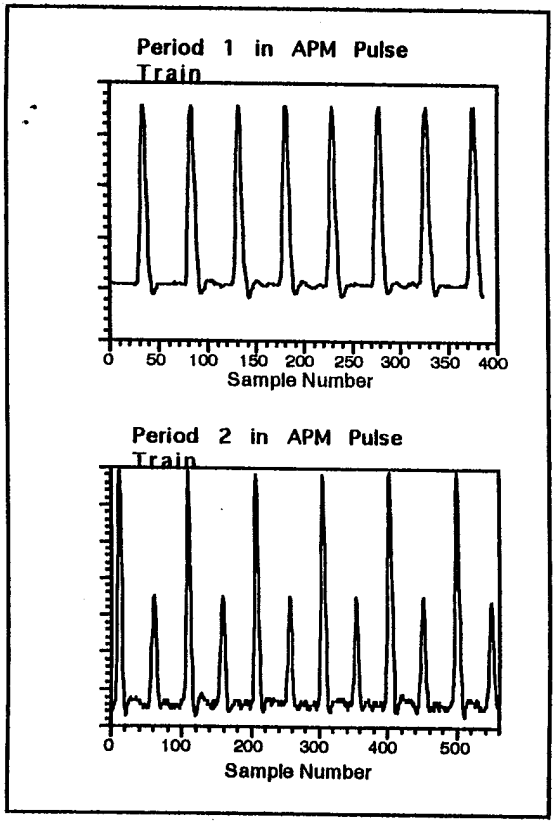

Cornell JSEP (F49620 93 C 0001) Task: J.P. Kruslus
Carrier Dynamics and Optical Processes in Ultra Fast C/S Photonic Devices

Objective
Explore Physics, Operation and Design of Photonic Devices

Approach
Fundamental Physics Based Modeling and Simulation (Self-Consistent Ensemble Monte Carlo Based)

Accomplishments
Formulation and Quantitive Understanding of Carrier Excitation/Relaxation in Femtosecond Dual Pulse Correlation Spectroscopy

Extension of Methodology to Ultra-Fast Optical Detectors

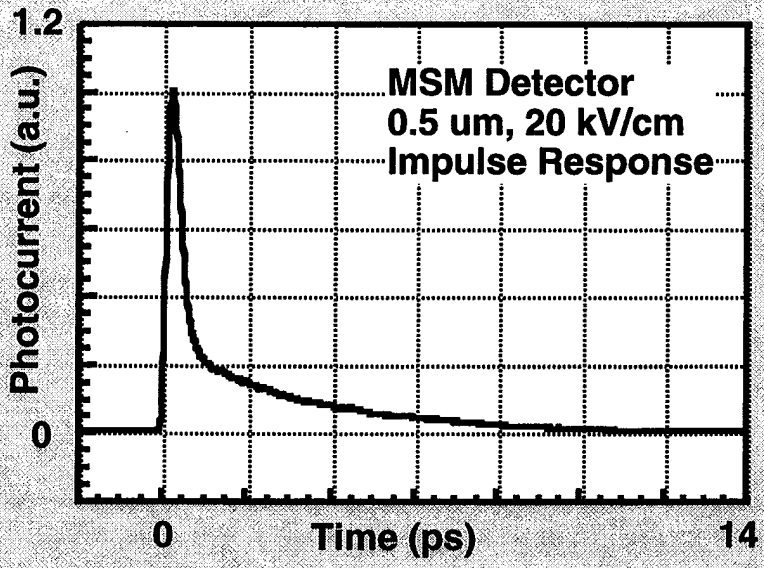

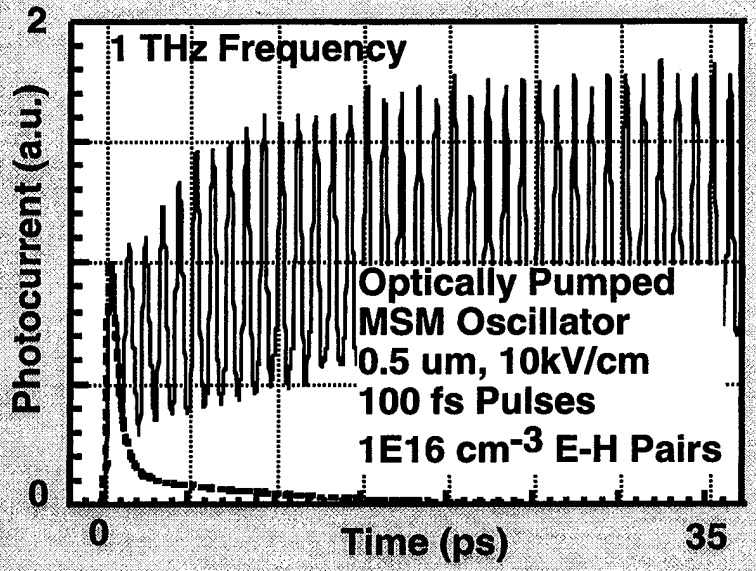

Cornell JSEP (F49620-93-C-001) Task: Yu-Hwa Lo
Strain-Compensated Multi-Quantum-Well Long Wavelength Surface Emitting Lasers

Objective: Demonstrating (1.3/1.55 μm) vertical-cavity surface-emitting laser using wafer bonded GaAs/AlAs Bragg mirrors and strain-compensated multi-quantum-wells

Key Features:

- Low threshold current
- Single longitudinal and lateral mode
- Wavelength tunability

Accomplishment:
Demonstrated 10 mA threshold for1.55 micron VC-SEL and single mode operation (>30 dB SMSR)

Device Structure

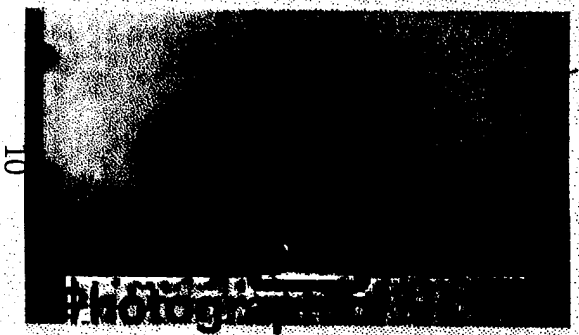

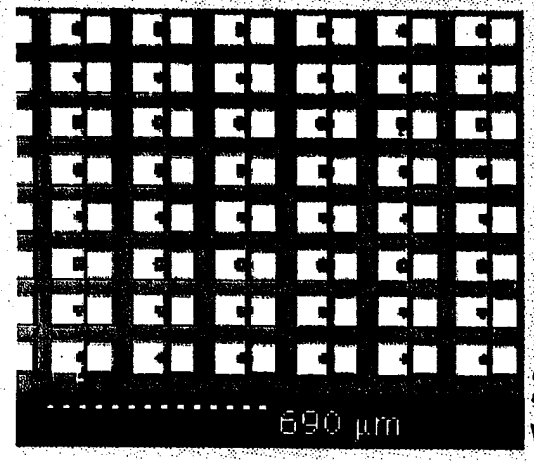

2D VCSEL array with wafer bonded mirrors

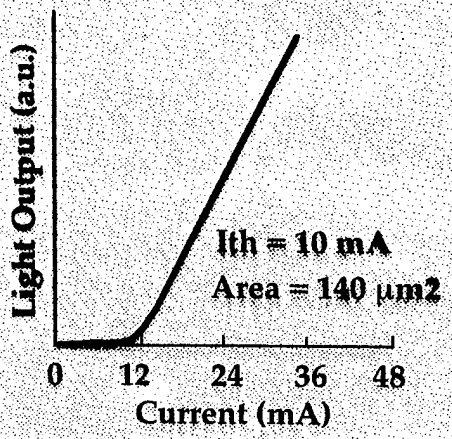

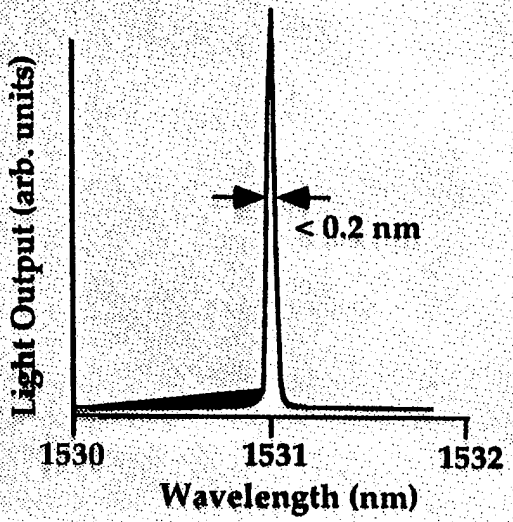

AlInAs/GaInAs High-Speed/Low Dark Current MSM Photodetectors with Copper Schottky Metal

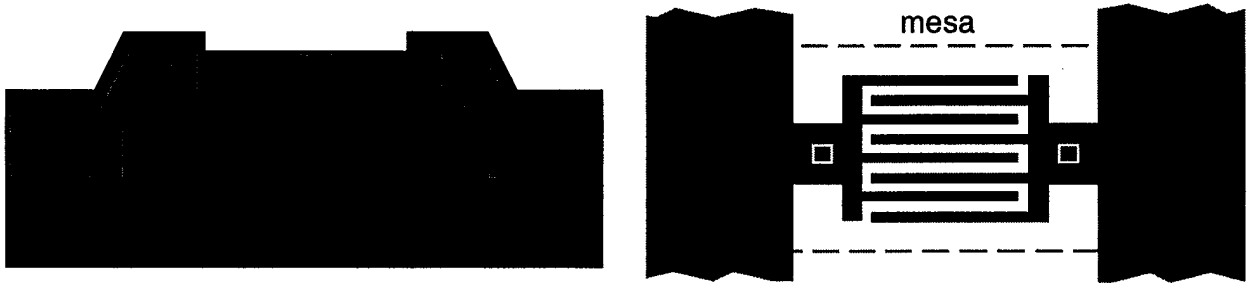

= Thick metal
= Polyimide
= Schottky metal

= AlInAs
= GaInAs
= InP

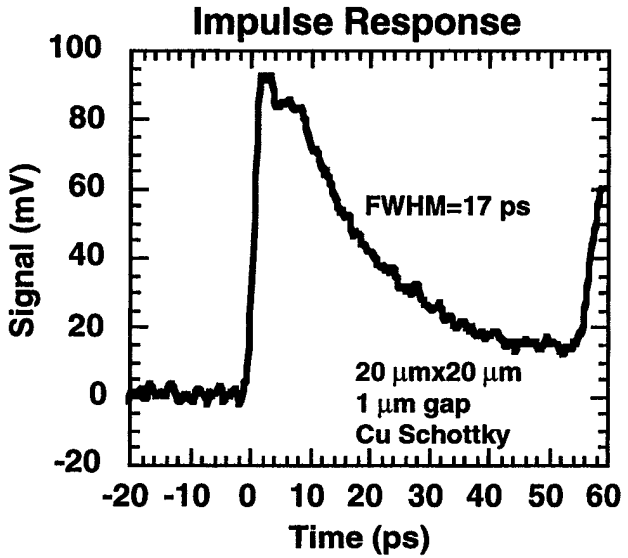

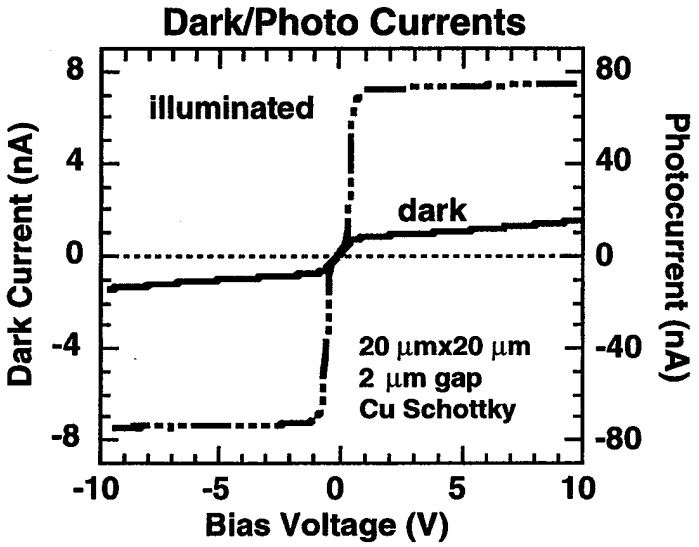

C. DESCRIPTION OF INDIVIDUAL WORK UNITS

OMVPE GROWTH OF III-V ALLOYS FOR NEW HIGH SPEED ELECTRON DEVICES

Task #1

Task Principal Investigator: **James R. Shealy**
Office: (607) 255-4657
Lab: (607) 257-3257
Fax: (607) 254-4777
email : shealy@ee.cornell.edu

OBJECTIVE

The overall program objective for this task is to extend the capabilities of our Flow Modulation Epitaxial (FME) processes to the synthesis of new semiconductor structures for high speed electronics and optoelectronics. This program has already helped establish two FME apparatus at Cornell, both of which are to be used in the new program. The first reactor is used to prepare new InP-based and GaAs-based heterostructures for application in mm-wave power-HEMTs and MSM photodetectors. The InP-based materials also include the preparation of new 1.3 μm laser structures. For HEMTs, our objective is to solve the two major problems encountered is the past program, the leaky AlInAs Schottky and buffer/substrate interface charge. Our approach is to investigate a pseudomorphic phosphide barrier as AlInAs is the source of both of these problems. For lasers, our objective is to optimize stress compensated GaInAsP superlattice structures for low threshold (and high T_0) 1.3 μm devices. The second FME machine is used to explore UV stimulated submicrometer selective growth. As the UV growth project is just underway we will not discuss this work in this report. Each of these JSEP activities provide leverage to other programs (and vice-versa) including our past interactions with Hanscom AFB and Hughes Research Labs on InP-based HEMTs, NSF, Raytheon and WPAFB on GaAs-based selective growth, and finally, the Tri-Service atomic scale imaging program at Cornell. In addition, we are extending the FME process to the nitride-based materials with new ARPA support.

DISCUSSION OF STATE-OF-THE-ART

The following discussion of the state-of-the-art represents selected results from the literature on the synthesis and analysis of InP-based materials and heterostructures as they relate to the past year's effort. The common theme for each materials system under investigation is the control of the arsenide to phosphide interface. All device structures investigated in this program incorporate these type of interfaces which are, in general, the most difficult to synthesize.

Structural Qualities of InP-based Heterostructures

The mixed crystal $Ga_xIn_{1-x}As_yP_{1-y}$ deposited on InP is an important materials system for optoelectronic devices.[1-3] Although Organometallic Vapor Phase Epitaxy (OMVPE) is typically the deposition method of choice for this system, the group V incorporation, especially in high bandgap (low As mole fraction) samples, is extremely sensitive to the deposition temperature.[4] Accordingly, it may be advantageous to find a replacement for the random alloy. By considering the quaternary as comprised of thin layers of lattice matched $Ga_{0.47}In_{0.53}As$ and InP, the random alloy may be synthesized with short period superlattices (SPSLs) or 'pseudo-alloys' containing GaInAs wells and InP barriers.[5] Any bandgap between those of GaInAs (1.67 μm) and InP (0.92 μm) may be obtained by varying the well and barrier layer thickness appropriately. Structures with a room temperature bandgap near 1.3 μm are particularly interesting from an application standpoint because of the importance of this wavelength to optical fiber based communications.

Since current flow occurs along the direction perpendicular to the layers in the pseudo-alloy, layer thickness must be adjusted such that carriers are not trapped in the high bandgap InP barriers. Appropriate layer thickness are determined by monitoring the superlattice miniband widths[6] as a function of superlattice structural parameters. Larger miniband widths correspond to increasing wavefunction overlap between adjacent wells and decreasing probability of carrier trapping. Accordingly, large miniband widths are desirable attributes in a pseudo-alloy. By comparing the electron ($0.079m_0$), light hole ($0.12m_0$), and heavy hole ($0.56m_0$) effective masses in GaInAs and InP,[7] we see that the heavy holes are the most strongly confined carriers in the pseudo-alloy. It follows that the narrowest minibands are associated with the heavy hole states and that the maximum barrier thickness is determined by the heavy hole miniband width. Kronig-Penney calculations using a four band model[8] indicate that both the InP and GaInAs thickness must be limited to 25-35 Å for heavy hole miniband formation to occur.

During the onset of GaInAs nucleation on InP, growth does not occur in the same fashion as it does in this bulk,[9,10] leading to interface related growth surface roughening.[8] Although this roughening may be smoothed by deposition of the subsequent InP layer, roughness can propagate from one interface to the next if the InP is not sufficiently thick.[11] In this situation, interface roughness is cumulative, leading to further modification of reactant incorporation relative to incorporation in the bulk and prohibiting synthesis of structures with a large number of periods. Because the superlattice stack must be thick enough to replace quaternary layers in device structures (e.g. ~0.1-0.2 μm for active or waveguide layers in 1.3 μm double heterostructure lasers),[12] the superlattice must contain at least 50 periods to constitute a viable pseudo-alloy. It has been demonstrated that the detrimental effects of growth surface roughening may be overcome by carefully adjusting the reactant fluxes in order

to synthesize lattice matched SPSLs with a large number of periods (> 100).[8] This is the approach adopted for growth of the pseudo-alloys investigated in this report.

PROGRESS

In this section, progress on the Flow Modulation Epitaxial growth and characterization of arsenide to phoshide interfaces is presented. Preliminary results on 1.3 μm lasers are also given.

FME Growth InP/GaInAs Pseudo-Alloys: Application to 1.3 μm Lasers

In this study, we synthesize a variety of GaInAs/InP SPSLs with periods and 300K bandgaps near 50 Å and 1.3 μm, respectively, in order to optimize growth of the pseudo-alloy. Samples were deposited at 600°C in a vertical barrel OMVPE reactor[13] and consisted of a 1500Å InP buffer followed by 50 repetitions of GaInAs and InP. Substrates were (100) n+ InP misoriented 0.3° toward the [110]. Source materials were triethylgallium (TEG), trimethylindium (TMIn), arsine (AsH_3), and phosphine (PH_3). The V/III ratio was fixed at 30 for the GaInAs and 275 for the InP.

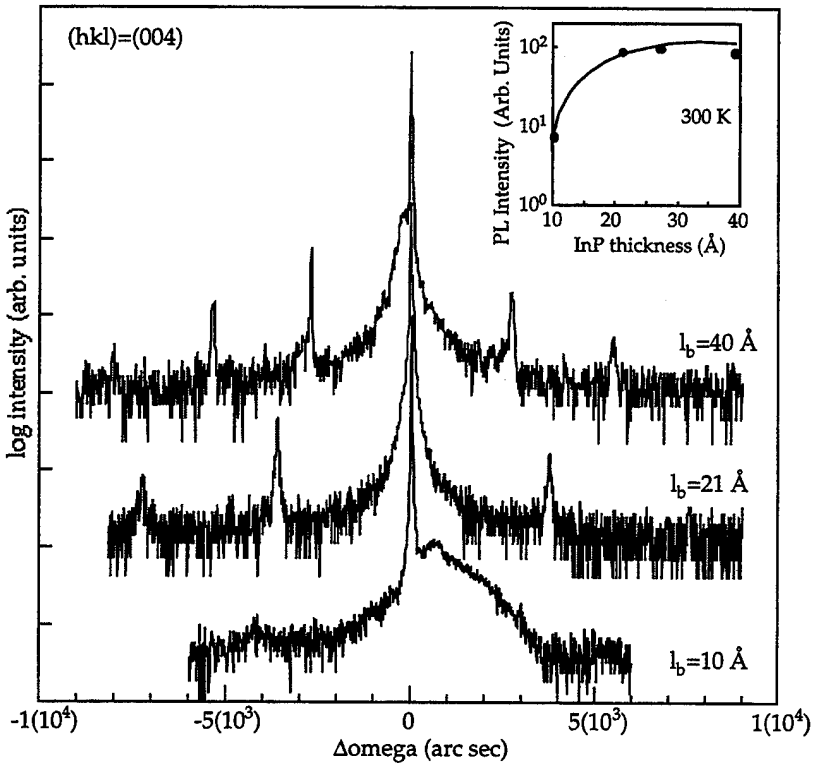

Figure 1. Effect of barrier thickness on structural quality of GaInAs/InP superlattices. Barrier thickness (superlattice period) is indicated to the right of each spectrum. Narrowing and strengthening of satellites as barrier thickness is increased demonstrates improving crystal quality. Inset shows effect of barrier thickness on 300K PL intensity for the same samples.

Growth rates ranged from 60-180 Å/min for the GaInAs and 23-70 Å/min for the InP. The interface formation technique, optimized to promote smooth interface formation, has been described previously.[8] Raman scattering, double crystal x-ray diffraction (DCXRD), photoluminescence (PL), and atomic force microscopy (AFM) were performed on the samples to assess their optical and structural quality. In addition, selected samples were examined with high resolution transmission electron microscopy (HRTEM) to confirm layer thickness as determined by DCXRD.

The InP's ability to smooth interfacial roughness is related to the prevailing growth kinetics. For example, as the growth temperature is increased, the metal species surface mobility similarly increases.[14] As long as growth proceeds in the mass transport limited regime, the InP becomes more effective at surface smoothing with increasing temperature. For each set of growth parameters, then, there is a different minimum InP thickness required to smooth the growth surface and prevent the accumulation of interfacial roughness. We sought to experimentally determine this minimum thickness for our process by holding the GaInAs thickness at 30 Å and then monitoring crystal quality as the InP growth time was altered. DCXRD spectra from SPSLs with 10, 21, and 39 Å thick barriers are shown in Fig. 1.

As evidenced by the reduction in intensity and increase in spectral width of the superlattice satellites in the 10 Å barrier sample relative to the thicker barrier samples, the structural quality deteriorates as the InP thickness is reduced from 21 to 10 Å. The 300K PL shows a similar trend, with the intensity decreasing rapidly as the InP thickness is reduced from 21 Å to 10 Å. From these results, we infer a minimum barrier thickness near 20 Å for growth of the pseudo-alloy under conditions used in this study.

To ascertain if pseudo-alloy synthesis was restricted to a rigid set of growth parameters, we varied the growth rate from 23 to 70 Å/min in a series of samples while holding all other parameters fixed. Growth times were adjusted as a function of growth rate so that the designed period would remain constant. As above, the intended well and barrier thickness were fixed at 30 Å and 22 Å, respectively. The normalized TEG flux (TEG flux divided by the TEG flux required to lattice match a bulk GaInAs layer at a given growth rate--see Fig. 3) was held at 0.55. DCXRD spectra from all three structures were similar to that of the 21 Å thick barrier sample shown in Fig. 1, confirming good structural quality. However, the average mismatch became increasingly negative as the growth rate was decreased. Raman scattering was used to investigate the cause of the mismatch trend. Since optic phonons are most sensitive to nearest neighbor interactions,[15] the longitudinal optic (LO) phonons sampled with Raman scattering can be used to probe interfacial layers in the pseudo-alloy. For samples that are not intermixed, LO phonons similar to those found in bulk superlattice constituents (here, GaInAs and InP) should

be observed. In contrast, interfacial layers give rise to distinct modes not present in the bulk constituents.[16,17] Raman spectra from the samples described in the previous paragraph are shown in Fig. 2.

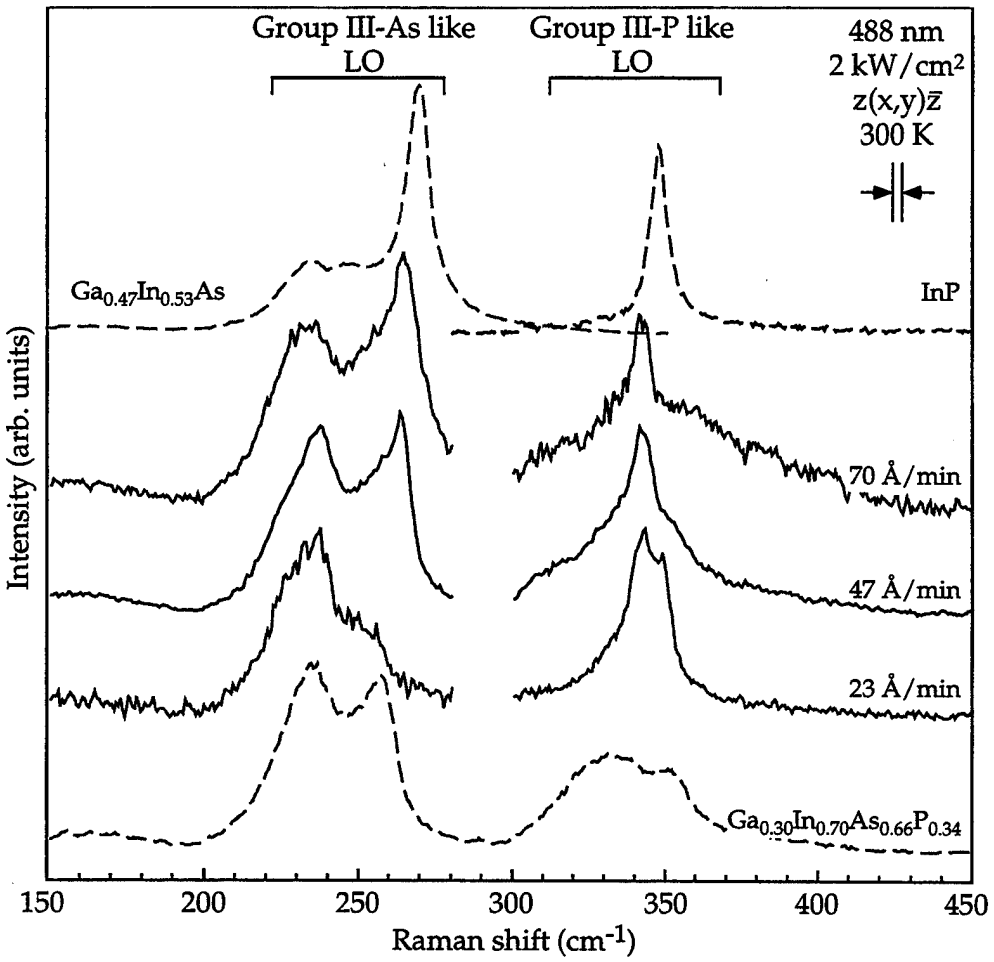

Figure 2. Identification of interfacial layers in GaInAs/InP superlattices with Raman scattering. Superlattice sample spectra (solid lines) are compared to spectra from bulk superlattice constituents and the corresponding mixed crystal quaternary (dashed lines). InP growth rate is given to the right of each superlattice spectrum. Experimental conditions are as indicated. Mode identification is explained in the text. Spectra have been normalized for comparison.

Spectra from GaInAs, InP, and $Ga_{0.30}In_{0.70}As_{0.66}P_{0.34}$ are also included for comparison. Two distinct phonon bands are observed, with the modes lying in the range from 230-270 cm^{-1} corresponding to group III-arsenic vibrations and the modes spanning the range from 300-360 cm^{-1} associated with group III-phosphorous vibrations.[18] As expected for a GaInAs/InP SPSL with a small degree of intermixing, distinct GaInAs- and InP-like modes are seen in the Raman spectrum from the highest growth rate sample. In contrast, the Raman spectrum from the lowest growth rate sample is more similar to the mixed crystal quaternary than to that of either of the intended superlattice constituent layers. When the Raman and DCXRD measurements are

considered simultaneously, the presence of a tensile strained GaInAsP layer whose thickness increases as the growth rate decreases is confirmed.

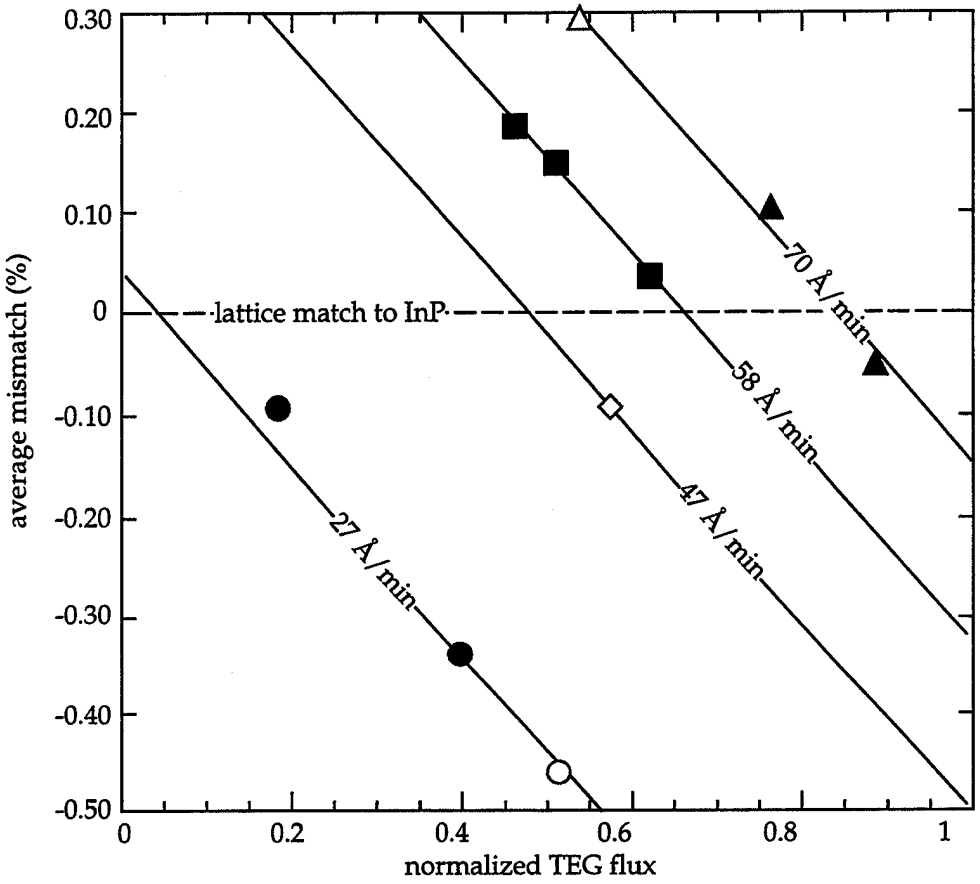

Figure 3. Lattice matching calibration of GaInAs/InP superlattices as a function of growth rate. Bulk InP growth rates are as indicated. Open symbols correspond to the samples whose Raman spectra are shown in Fig. 2. Solid lines are guides to the eye.

Simulation of the DCXRD data fix its location at the barrier to well interface and demonstrate that it is tensile strained due to enhanced Ga incorporation at this interface. Its behavior with growth rate is explained as follows: As the growth rate is decreased, the time required to change growth from InP to GaInAs is increased. As a result, the thickness of any GaInAsP interfacial layer formed during this transition time increases as the growth rate decreases. In order to determine if the growth rate related layer intermixing precluded the formation of high quality, lattice matched samples, we varied the TEG flux for four different growth rates to obtain experimental mismatch calibration curves for the 1.3 μm bandgap pseudo-alloy. As shown in Fig. 3, the normalized TEG flux required to preserve average lattice match was reduced in a repeatable and predictable fashion as the growth rate was lowered. Regardless of the growth rate and the corresponding degree of intermixing, the flux could always be adjusted appropriately for growth of lattice matched structures with good optical and structural quality. In all cases, the 300K bandgap of the lattice

matched samples was near 1.3 μm with full-width at maxima of 60-70 meV, comparable to the values expected from the corresponding mixed crystal. Because our results are repeatable over a wide range of growth rates, a fundamental growth parameter, they are general to the OMVPE growth technique and are not limited to the particular reactor geometry.

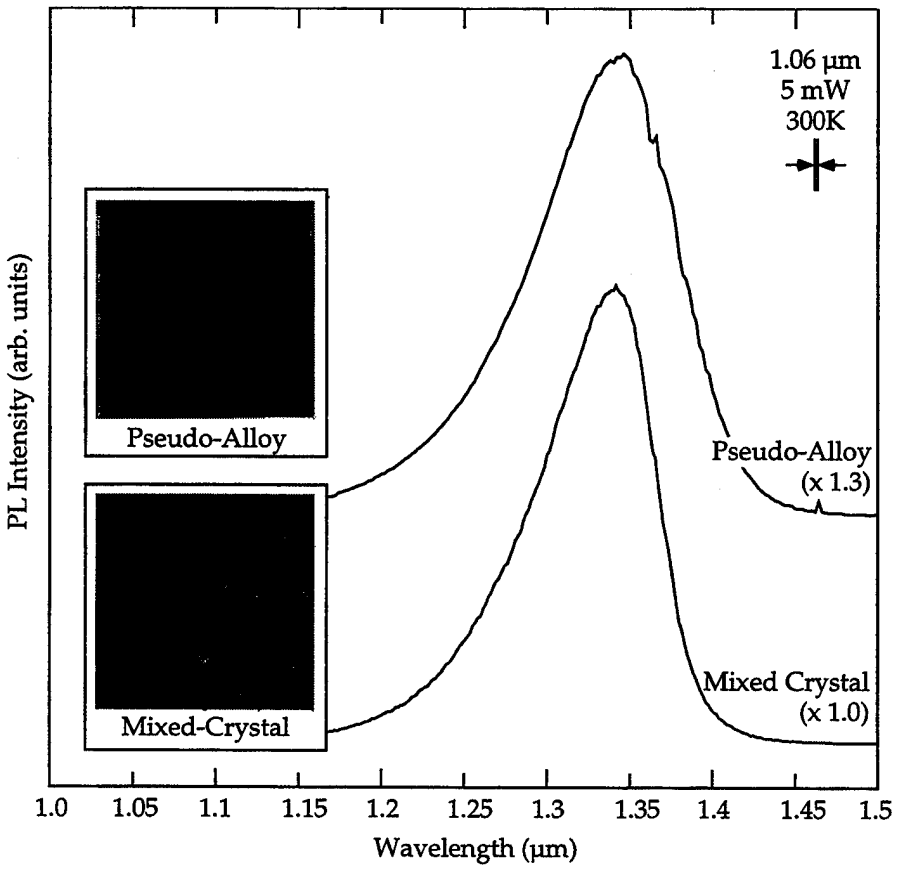

Figure 4. Comparison of pseudo-alloy and mixed crystal quaternary optical properties and surface morphology. Experimental conditions are as indicated. PL spectra have been normalized, with normalization factors given in parenthesis. Inset shows 10 μm x 10 μm AFM surface micrographs. Well defined lines are monolayer steps.

In Fig. 4, we compare the optical and structural properties of a pseudo-alloy (52 Å period) with those of the corresponding random alloy, $Ga_{0.30}In_{0.70}As_{0.66}P_{0.34}$. Effective growth rates were 0.47 μm/hr and 0.89 μm/hr for the pseudo- and random-alloys, respectively, with the SPSL growth rate reduced relative to that of the random alloy because of 10 sec growth interruptions employed between each layer in the superlattice.[8] The 300K PL peaked near 1.34 μm for both samples, and the intensity and spectral width were similar. Furthermore, the surface morphology of the pseudo-alloy, characterized by monolayer steps in the AFM micrographs, is comparable to that of the mixed crystal.

Finally, we incorporated the pseudo-alloy in the active region of a broad area superlattice separate confinement heterostructure (SL-SCH) laser. This study represents the first such attempt to do so. The superlattice lasers consists of InP cladding regions (1.25 μm on top and 0.5 μm below the active region), and 0.12 μm of GaInAsP separate confinement regions (with a 1.1 μm bandgap). A 750 Å InP spacer layer was inserted between the p-type, Zn-doped cladding region and the active region to prevent Zn diffusion into the active region during growth. Threshold current for an unoptimized structure containing 25 periods of the pseudo-alloy in the active region were as low as 3 kA/cm^2 at room temperature as shown in Fig. 5.

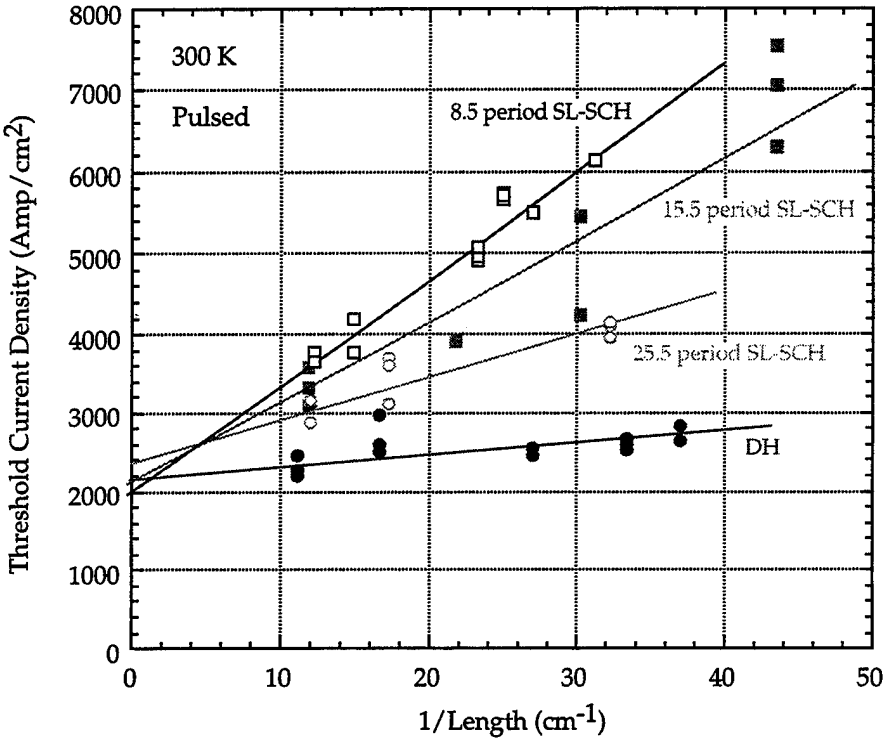

Figure 5. Threshold current density versus inverse cavity length of broad stripe 1.3 μm lasers with superlattice active regions compared against a simple InP/GaInAsP DH structure with a 2000 Å thick active region.

In this figure, the threshold current density is plotted versus inverse cavity length. The active gain region thickness is obtained by multiplying the number of superlattice periods shown in the figure by the period used (52 Å in these structures). For comparison, test data on a DH structure with a 2000 Å thick active region is also given. For devices with a bulk active region, we expect the slope of the lines drawn for each structure to be inversely proportional to the differential gain-confinement factor product.[19] As the number of superlattice periods increases the confinement factor increases with the differential gain roughly constant. From this model, we expect the slope of the curves to scale inversely with the number of periods in the superlattice gain region. For a multi-quantum well device the dependence on the slope

changes to scale roughly with the quantum well dimension which is constant in these superlattice devices (the confinement factor dependence is canceled as it scales with the number of wells). This model which ignores gain saturation predicts a weak dependence on the slope (J_{th} vs. 1/L). The superlattice devices are somewhere between these two extremes as evidenced by the data shown in Fig. 5.

Finally, if the superlattice devices are compared against a similar SCH structure with a bulk GaInAsP active region (1500 Å in thickness), we obtain lasers with roughly one half the threshold current (as low as 1500 amps/cm^2 for the bulk active region). Although the superlattice devices exhibit a larger threshold current density, their temperature performance is of great interest for applications in fiber communications. We are currently evaluating these device's temperature coefficient (T_0) under pulsed conditions. In any event, this demonstration is an important proof of principle (and the first) that the pseudo-alloy is a viable candidate for replacement of the 1.3 μm bandgap mixed crystal quaternary.

SCIENTIFIC IMPACT OF RESEARCH

Our Flow Modulation Epitaxial process has solved some very basic problems in the OMVPE growth of As-to-P interfaces. We have demonstrated the shortest period superlattice built to date with the GaInAs/InP and incorporated these structures in new 1.3 μm lasers. If improved temperature performance is observed in superlattice devices as we expect, they will have a large impact on fiber-based communication systems.

DEGREES AWARDED

Ph.D., D.T. Emerson (August 1995)

REFERENCES

[1] R. Saxena, V. Sardi, J. Oberstar, L. Hodge, M. Keever, G. Trott, K.L. Chen, and R. Moon, J. Crys. Growth **77**, 591 (1986).

[2] M. Silver and E.P. O'Reilly, IEEE J. Quantum Elec **31**, 1193 (1995).

[3] R.E. Nahory, M.A. Pollack, and W.D. Johnston, Jr., Appl. Phys. Lett. **33**, 659 (1978).

[4] R.M. Lum, M.L. McDonald, E.M. Mack, M.D. Williams, F.G. Storz, and J. Levkoff, J. Elec. Mat. **24**, 1577 (1995).

[5] F. Capasso, H.M. Cox, A.L. Hutchinson, N.A. Olsson, and S.G. Hummel, Appl. Phys. Lett. **45**, 1193 (1984).

[6] S. Wang, Semiconductor Fundamentals.

[7] S. Adachi, J. Appl. Phys. **53**, 8775 (1982).

[8] D.T. Emerson, K.L. Whittingham, and J.R. Shealy, Inst. Phys. Conf. Ser. **141**, 155 (IOP Bristol, 1995).

[9] N. Yokouchi, Y. Inaba, T. Uchida, T. Miyamoto, K. Mori, F. Koyama, and K. Iga, J. Crys. Growth **136**, 302 (1994).

[10] W. Seifert, J.-O. Fornell, L. Ledebo, M.-E. Pistol, and L. Samuelson, Appl. Phys. Lett. **56**, 1128 (1990).

[11] C. Rigo, A. Antolini, C. Cacciatore, C. Coriasso, L. Lazzarini, and G. Salviati, J. Crys. Growth **136**, 293 (1994).

[12] Y. Itaya, Y. Suematsu, S. Katayama, K. Kishino, and S. Arai, Jpn. J. Appl. Phys. **17**, 1795 (1979).

[13] B.L. Pitts, M.J. Matragrano, D.T. Emerson, B. Sun, D.T. Ast and J.R. Shealy, Inst. Phys. Conf. Ser. **136** 619 (IOP Bristol, 1993).

[14] M. Shinohara, M. Tanimoto, H. Yokoyama, and N. Inoue, Appl. Phys. Lett. **65**, 1418 (1994).

[15] C. Colvard, T.A. Gant, M.V. Klein, R. Merlin, R. Fischer, H. Morkoc, and A.C. Gossard, Phys. Rev. B **31**, 2080 (1985).

[16] J. Geurts, D. Gnoth, J. Finders, A. Kohl, and K. Heime, Phys. Stat. Sol. **152**, 211 (1995).

[17] H. Asahi, T. Kohara, R.K. Soni, K. Asami, S. Emura, and S. Gonda, J. Crys. Growth **127**, 194 (1993).

[18] R.K. Soni, S.C. Abbi, K.P. Jain, M. Balkanski, S. Slempkes, and J.L. Benchimol, J. Appl. Phys. **59**, 2184 (1986).

[19] Y-H Lo, Private Comm.

JSEP PUBLICATIONS

1. "Optical and Structural Characterization of Arsenide/Phosphide Interfaces Formed by Flow Modulation Epitaxy," D.T. Emerson, J.A. Smart, K.L. Whittingham, E.M. Chumbes, and J.R. Shealy. Invited Talk, Diagnostics for Semiconductor Materials Processing, Fall 1995 MRS Meeting, Boston, MA, November 1995.

2. "Effect of Phosphorus Composition on the Structural Quality of GaInP/GaAsP Short-Period Superlattices," K.L. Whittingham, D.T. Emerson, J.R. Shealy, M.J. Matragrano, and D.G. Ast, *Appl. Phys. Lett.* **67** (25), 18 December 1995.

3. "Structural Investigation of Short Period GaInAs/InP Superlattices," D.T. Emerson and J.R. Shealy, accepted for publication in *Appl. Phys. Lett.*, May 1996.

4. "Synthesis of InP-based 1.3 μm Bandgap Pseudo-Alloy by Organometallic Vapor Phase Epitaxy," Emerson and J.R. Shealy, submitted for publication in *Appl. Phys. Lett.*, May 1996.

5. "Flow Modulation Growth and Tellurium Doping of $Al_{0.48}In_{0.52}As$/InP for InP-based HEMTs," D.T. Emerson, V.A. Williams, J.R. Shealy, and J.B. Shealy, to be presented, Electron Materials Conference, June 1996.

RELATED PUBLICATIONS

1. "III-V Materials Synthesis at Cornell Using Novel Processes," Invited talk, AT&T Bell Laboratories, Murray Hill, NJ, June 29, 1995.

2. "Selective Growth of GaP on Si by Metal Organic Vapor Phase Epitaxy," J.S. Lee, J. Salzman, J. Ballantyne, D. Emerson, and J.R. Shealy. Diagnostics for Semiconductor Materials Processing, Fall 1995 MRS Meeting, Boston, MA, November 1995.

3. "New Approach to the Synthesis GaN Boules and Homoepitaixal Growth," Invited talk, Third St. Louis Workshop on Wide Bandgap Nitrides, St. Louis, MO, March 13, 1996.

4. "Direct Bandgap Structures on Nanometer-Scale, Micro-Machined Silicon Tips," J.R. Shealy, K.L. Whittingham, B.L. Pitts, N.C. McDonald, and Y. Xu, accepted for publication, *Appl. Phys. Lett.*, 1995.

5. "Selective Growth of GaP on Si by MOCVD," J.Lee, J. Salzman, D. Emerson, J. Ballantyne, **J.R. Shealy**, submitted for publication, *Journal of Crystal Growth*, Nov. 1995.

6. "Anistopic Strain Relaxation of GaInP Epitaxial Layers in Compression and Tension," M.J. Matragrano, D.G. Ast, J.R. Shealy and V. Krishnamoorthy, accepted for publication, *Journal of Applied Physics*, 1996.

7. "Measurement of the Mean Free Path of Dislocation Glide in the InGaAs/GaAs Materials System," M.J. Matragrano, D.G. Ast, G.P. Watson, and J.R. Shealy, *J. Appl. Phys.* **79** (2), 15 January 1996.

FEMTOSECOND LASER STUDIES OF ULTRAFAST PROCESSES IN COMPOUND SEMICONDUCTORS

Task #2

Task Principal Investigator: **C. L. Tang**
Office: (607)255-5120
Fax: (607) 254-4565
E-mail: cltang@ee.cornell.edu

OBJECTIVE

The objective of this task is to develop new femtosecond sources and measurement techniques and to apply these to the study ultrafast processes in semiconductors and related quantum well structures. Current emphasis is on applying the high repetition rate all-solid-state femtosecond sources in the important 3 to 5 μm range and the blue-green range first developed in our laboratory to the study of the relaxation dynamics of non-equlibrium carriers in elemental and compound semiconductors and quantum well structures. Materials under study are HgCdTe and InGaAs.

DISCUSSION OF STATE-OF-THE-ART

Time resolved spectroscopy has been an important technique for the study of ultrafast processes in atoms, molecules, and semiconductors. With the development of broadly tunable sources such as the mode locked Ti:sapphire ($Ti:Al_2O_3$) laser, and the high repetition rate, femtosecond optical parametric oscillator (fs-OPO), there are now a wide range of ultrafast phenomena that can be studied. One major advantage of the fs-OPO is its broad tunability, systems based on $KTiOPO_4$ (KTP), and its isomorphs have successfully generated femtosecond pulses spanning the near-infrared spectral range.

There is considerable interest in the 3-5 μm region for the study of molecular processes such as vibrational relaxation, and for various semiconductor phenomena such as band-to-impurity transitions, intraband free-carrier absorption, intra valence band transitions, inter suband transitions in quantum wells and coherent phonon effects. Until recently, short pulse generation in this region has required the used of difference-frequency mixing (DFM) or a free-electron laser. While such schemes offer tunability in the 3 - 5 μm range and beyond, they require complicated experimental systems. In addition, the repetition rate is often limited to the kHz range or less, and in the case of DFM, the available output powers are limited to a few

μW. We have recently developed a Ti:Al_2O_3 laser pumped fs-OPO based on the nonlinear material potassium niobate ($KNbO_3$). We have demonstrated that this fs OPO can operate to 5.2 μm at an average power level of over 20 mW at 10^8 Hz repetition rate. This represents a significant improvement over existing systems, in terms of wavelength, power, and repetition rate. With such a source, it is now possible to study the ultrafast relaxation dynamics of hot carriers in such important infrared materials as HgCdTe, InSb, GaSb, and InGaAs using methods that have previously been developed and extensively applied to such materials as GaAlAs. The range of materials and the type of processes that could be studied previously was limited by the available femtosecond sources to around 630 nm from the Rh6G dye laser, 750 to 900 nm from the Ti:sapphire laser, and 1.2 to 1.5 μm from the color center lasers. The limited wavelength range of such sources also limits the states that could be studied in each material. The broad tunability of the fs OPO will allow well separated states in each material to be excited and probed simultaneously. The ability to probe different states simultaneously is particularly important in order to identify the origins of different relaxation processes.

In the types of II-VI and III-V compound semiconductors of interest, it is known that there are a number of possible scattering processes that contribute to the energy and momentum relaxation of highly excited carriers including intravalley and intervalley acoustic and optical phonon scattering, electron-electron and electron-hole scattering, and scattering from ionized impurities. With the broad tunability and well synchronized femtosecond pulses from the pump laser and the OPO, it is now possible to monitor not only the initially excited states, as was generally done in previous studies, but also a variety of final states simultaneously. The results will help to elucidate the detailed physics involved.

The output of the fs OPO could also be efficiently doubled and mixed with the pump light to convert the broadly tunable output into the visible region. This will allow us probe a broad range of states in such important material InP. In particular, it can cover those central valley states that are above and below the L- and X-valley minima. This will help to isolate the intervalley scattering processes and determine the corresponding deformation potential in such a material. The information on such important parameters is very limited at the present time.

PROGRESS

As a part of our effort to extend the tunable femtosecond measurement capability into the important 3 - 5 μm range, we have demonstrated for the first time the operation of a high average power, high repetition rate

femtosecond $KNbO_3$ OPO that operates with a continuous tuning range from 2.3 to 5.2 μm. The corresponding idler pulse durations were determined using cross-correlation techniques and pulses as short as 60 fs were measured in the infrared.

We have also demonstrated efficient doubling and up-conversion of the KTP fs OPO down to the 520 nm range using $LiIO_3$. We now have basically continuous spectral coverage from the visible to 5.2 μm in the femtosceond time domain.

As shorter pulses over an ever wider range of wavelengths are generated, it is equally important to have a more reliable data reduction method so that the correct relaxation time constants can be extracted. The problem is complicated by the fact that the measured time dependence is often the result of several competing relaxation processes. For example in the case of relaxation of hot carriers in semiconductors, or of large molecules, there can be a large number of decay components. In addition, there may be other time dependent experimental artifacts present in the data. When the number of components is not known, or if the number is large, the conventional nonlinear fitting procedure is not reliable. An alternative approach uses a relatively recent technique based on linear prediction. This enables the problem to be formulated in such a way that a linear least-squares procedure, based on singular value decomposition (or LPSVD procedure) can be used to analyze the data reliably. A study was carried to look in detail at how the LPSVD technique can be applied to data from femtosecond time-resolved spectroscopy experiment. This technique will allow us to isolated different relaxation paths in the materials being studied. It is being applied to the experimental data and InP and HgCdTe described below.

We have recently obtained a sample of $Hg_{0.55}Cd_{0.45}Te$ transparent to about 2.8 μm from AF Phillips Lab. Work is under way to make a preliminary study of this material using the fs OPO source and the method of data analysis recently developed in our laboratory. We will measure the ultrafast relaxation time of hot electrons excited in various states in the central valley. One question that had also not been addressed in earlier similar studies on GaAlAs was the role of plasmon scattering in the relaxation of hot carriers. By varying the concentration of the excited carriers, we should be able to identify the contribution of this particular relaxation mechanism to the total decay rate. If additional samples with different doping species and doping densities can be obtained, we should also be able to determine the scattering rates due to ionized impurities. By varying the excited states across various satellite valley minima, we should be able to isolate in addition the contributions of the intervalley scattering processes and determine the corresponding deformation potential parameters.

Using the hot luminescence up-conversion technique and the doubled and upconverted outputs of the mode-locked Ti:sapphire laser and the fs OPO, we are also collecting data on the hot luminescence from InP and InGaAs. We will be able to explore in particular the initial states in the central valley that have energies that bracket various satellite valley minima and the final states throughout the central valley. Tracking the time dependencies of the carriers entering and leaving these should provide a much clearer picture of the relaxation dynamics of the hot carriers.

SCIENTIFIC IMPACT OF RESEARCH

The tunable femtosecond sources and measurement techniques developed should be of great use to others in the scientific community. The results obtained on the dynamics of nonequilibrium carriers in compound semiconductors and structures are of fundamental importance to the understanding of the physics and the design of ultra-high speed semiconductor electronic and optical devices.

DEGREES AWARDED

None

REFERENCES

None

JSEP PUBLICATIONS

1. "A high repetition rate, femtosecond optical parametric oscillator based on $KNbO_3$", D. E. spence, S. Wielandy, C. L. Tang, C. Bosshard, and P. Gunther, Optics Letters 20, 680-682(April 1, 1995).

2. "Characterization and applications of high repetition rate broadly tunable femtosecond optical parametric oscillators", D. E. Spence and C. L. Tang, J. of Selected Topics in Quant. Elect. , Vol.1, 31(April 1995).

3. "High average power, high repetition rate femtosecond pulse generation in the 1 - 5 μm region using an optical parametric oscillator", D. E. Spence, S. Wilandy, C. L. Tang, C. Bosshard, and P. Gunter, App. Phys. Letters 68, 452(22 Januray, 1996).

4. "Broadly tunable high-repetition rate femtosecond sources and transient coherent wavepacket oscillations", C. L. Tang, Laser Physics, Vol.5, No.3, pp.1-6 (1995, Moscow, Russia)

5. "Cross-correlation measurements on a high repetition rate, femtosecond optical parametric oscillator", D. E. Spence, P. E. Powers, and C. L. Tang, Opt. Comm. **118**, 69-73(1995)

6. C. L. Tang and L. K. Cheng, *Fundamentals of Optical Parametric Processes and Oscillators* (Harwood Academic Press, 1996).

7. "Ultrashort pulse phenomena", C. L. Tang and D. E. Spence, to be published in Enclopedia of Applied Physics, eds. G. L. Trigg and E. S. Vera, (VCH Publishers)

JSEP PRESENTATIONS

1. "Broadly tunable high repetition rate femtosecond OPO using KNbO3", D. E. Spence, S. Wielandy, C. L. Tang, C. Bosshart, and P. Gunter, CLEO '95 Baltimore, MD, May 23, 1995.

2. "Broadly tunable high-repetition rate femtosecond sources and ultrafast optical correlation spectroscopy", C. L. Tang, invited talk at 2nd Mediterranean Workshop and Topical Meeting "Novel Optical Materials and Applications" -NOMA, May 28 - June 2, 1995, Cetraro, Italy.

3. "High repetition rate broadly tunable femtosecond optical parametric sources", C. L. Tang, invited talk at ICONO '95, June 26 - July 2, 1995, St. Petersburg, Russia.

4. "Optical parametric processes and broadly tunable femtosecond sources", C. L. Tang, invited talk, Second International Conference on Organic Nonlinear Optics, July 23 -26, 1995, Kusatsu , Gumma, Japan.

HIGH SPEED CARRIER RELAXATION PROCESSES IN OPTOELECTRONIC DEVICES

Task #3

Task Principal Investigator: **Clifford R. Pollock**
Office: (607) 255-3989
Fax: (607) 254-4565
e-mail: cpollock@ee.cornell.edu

OBJECTIVE

In the last year we have had three research objectives: 1) to obtain real data on high speed carrier relaxation processes for comparison with the Monte-Carlo simulations produced by Prof. Krusius group, 2) to use the ultrashort pulses generated by our lasers to the testing of an all-optical modulator being developed at the Air Force Rome Labs, and 3) to identify the chaotic operation of a high speed laser, with the aim of mapping out the chaotic regimes and ultimately to control the chaotic behavior.

DISCUSSION OF STATE-OF-THE ART

Using pulse-probe techniques, the high speed dynamics of electrons in GaAs and InGaAs have been rigorously studied over the past decade. Recent work has focussed on the new near infrared femtosecond sources that are now available. Using a color center adaptive pulse mode-locked (APM) laser identical to what we have in our lab, Sucha and Chemla[1] studied time resolved measurements of carrier dynamics in bulk and quantum wells InGaAs using differential absorption spectroscopy. They observe carrier thermalization time at 200-300fs, independent of sample thickness or bulk versus QWs. They found that the efficiency of screening relative to phase space filling is larger in the bulk than in quantum wells. Tomita and Shah [2] focused on hole dynamics in n-doped GaAs/AlGaAs QW's in what they believe to be the first unambiguous study of initial hole relaxation in GaAs QW's. They show that holes are non-thermal for approximately 800 fsec after excitation and they determine hole-electron energy loss rates, which they attributed to Coulomb interaction.

Davidson, Compton, and Wise [3] studied intraband relaxation of minority electrons in heavily carbon-doped GaAs, finding a strong dependence on doping level. Heavily doped p-type GaAs is important in it's use in the base region of npn heterojunction bipolar transistors. They attribute the dependence to electron-hole scattering, with electrons relaxing into states created by band-gap renormalization and band tailing. In our current JSEP

work, Cohen [4] measured the electron relaxation in n-doped InGaAs as a function of excitation energy. This work is described below.

In 1990, Edward Ott, Celso Grebogi, and James Yorke (OGY) [5] at the University of Maryland demonstrated that chaotic systems can be controlled by means of small steering perturbations. The OGY algorithm was first implemented experimentally by Ditto [6] at the Naval Surface Warfare Center in order to control the chaotic behavior in a magnetoelastic ribbon vibrating at 0.85Hz. Due to the long oscillation period, there was ample time to calculate by computer the required feedback factor. Experimentally, it is complicated and time consuming to calculate the OGY-required perturbations necessary to stabilize the unstable periodic orbits. Hunt at Ohio University [7] successfully adapted the OGY algorithm for a 53kHz sine-wave-driven diode resonator using a technique known as occasional proportional feedback (OPF). By using the constant amplification factor instead of the factor calculated by OGY, the frequency range of control was extended. However, advantages gained by this simplification are offset by a difficulty in predicting which orbit will be controlled.

Using Hunt's OPF technique, Roy [8] at Georgia Tech controlled chaos in a diode-laser-pumped Nd:YAG laser which contains a KTP crystal in the cavity as a second harmonic generator. For certain rotational orientations of the KTP and YAG crystals the system becomes chaotic. The controlling feedback was obtained by sampling the laser's output intensity at the relaxation oscillation frequency of 118kHz. The amplified difference between this intensity and the desired intensity was then used to modulate the control signal to the diode laser pump. In this manner, orbits up to period 9 were stabilized for durations of several minutes. Bielawski et al. at the University of Lille [9] stabilized the unstable periodic orbits in a Nd-doped optical fiber laser that was operating at 15kHz.

The above work in controlling chaos has been applied to relatively slow systems in which analog electronics are capable of evaluating and implementing any required perturbations. An avenue for controlling fast dynamical systems has been theoretically explored by Pyragas [10] at the University of Tubingen. He showed that low period UPOs could be stabilized by continuously applying feedback obtained by subtracting a dynamical variable of the system from the same output signal, but time-delayed by the period of the desired UPO. Experimental demonstration of the time-delayed feedback algorithm was subsequently performed by Pyragas and Tamasevicius [11] to stabilize periods 1 through 4 in a 4 MHz driven nonlinear oscillator composed of a tunnel diode, inductor and capacitor. This scheme has also been applied by Glorieux et al. [12] in order to control unstable periodic orbits in a carbon dioxide laser that typically operates at the relaxation oscillation frequency of 400 kHz.

PROGRESS

Our work in the last year has concentrated on completing the detailed measurement of carrier relaxation in In0.53Ga0.47As, and the correlation of these measurements with an inclusive theoretical model. Using an additive pulse modelocked (APM) NaCl laser operating with 0.8 eV pulses, we have probed this n-type doped semiconductor near the Fermi level, and thereby created a small perturbation to the majority carrier density. Graduate student David Cohen performed all of this experimental work, and also assembled a theory of carrier relaxation including carrier-carrier scattering and carrier-phonon interactions.

Experimentally, tunable incident pulses excite carriers at different conduction band excess energies. Figure 1 shows the temporal relaxation of the relative transmission for three specific cases. Results for smaller excess energies correspond to wider temporal profiles, indicating the presence of a slow thermalization process. Experimental data was analyzed in conjunction with members of Prof. Peter Krusius' group, who used Monte-Carlo techniques to explore hte details of the microcopic carrier physics. From their analysis, two exponential processes were gleaned from the data. The fast process, with a time constant of about 100 fs, corresponds to rapid thermalization primarily by intraband Coulomb carrier-carrier interactions. The second and more interesting process has a time constant of about 1 - 1.3 ps, and results from the equilibration of a perturbed, Fermi-Dirac type conduction band distribution. This process is thought to correspond to a fast change in distribution temperature: temperature change on a time scale which has yet to be thoroughly studied. The presumed reason for the slower relaxation at lower excess energy is due to the fact that the 'hot' electrons do not have sufficient energy to create LO phonons, so they cannot shed their energy in this channel. They must rely energy transfer to acoustic phonons [13]

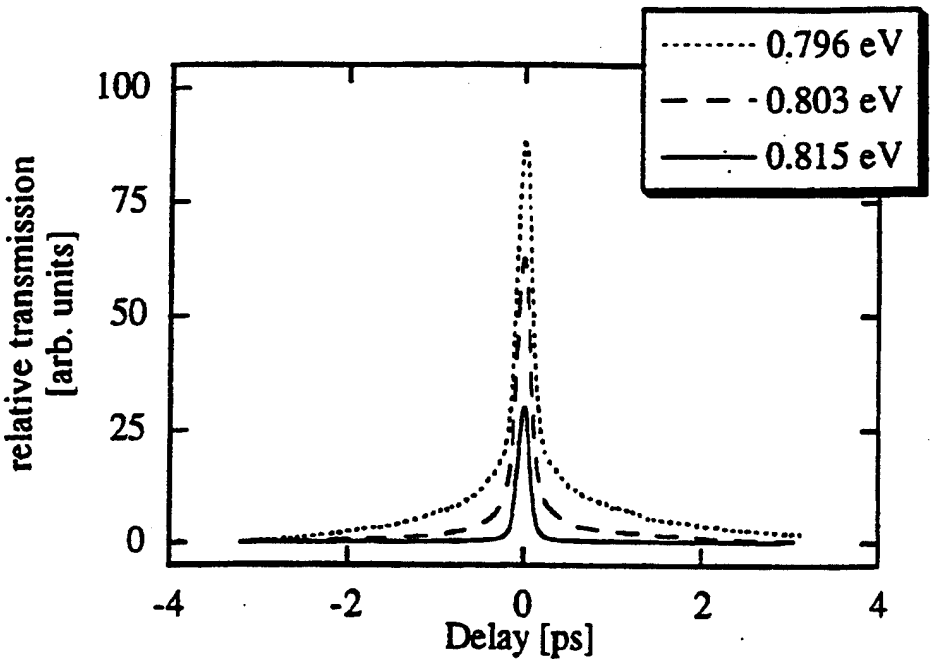

Figure 1. Two-pulse autocorrelation data from a n-InGaAs sample, probed at three different photon energies.

In this work, hole scattering events were neglected due to the large density of heavy-hole states, and resulting slow time constant of hole processes. Indeed, in most current semiconductor pump-probe experiments, hole dynamics are avoided. For this reason, little has been revealed concerning excited hole relaxation.

In addition to these areas of study, we have fostered continuing efforts with two Air Force Laboratories. First, we have been collaborating with Mark Krol et. al at the Rome Laboratory Photonics Center, Griffiss Air Force Base. This group has been exploring hole tunneling in asymmetric double quantum well (ADQW) structures. We are collaborating using the modelocked Cr:Forsterite laser as a pump/probe source for the DQW setup. Previously, the Rome Laboratory group used a Ti:Sapphire pulsed pump (100 fs at 844 nm) which generated excess carriers in both the narrow and wide quantum wells, and a CW Cr:Forsterite probe (tunable from 1.22 to 1.29 μm), which was tuned to the narrow well heavy hole energy at the Gamma point (Fig. 2, HHN1). Excited holes in the narrow well decay to the Gamma point of HHN1, and also tunnel to the wide well heavy hole band (HHW1.) Krol et. al found that low excited carrier densities yield a fast, single-exponential decay, corresponding to hole tunneling from the narrow to the wide well. Higher excited carrier densities, on the other hand, reveal a slow decay component which pertains to holes decaying to the Gamma point in the narrow well.

This component is seen only at higher carrier densities because the heavy hole band in the wide well saturates, and further tunneling from the narrow to the wide well is reduced, forcing holes to slowly decay to the narrow well Gamma point.

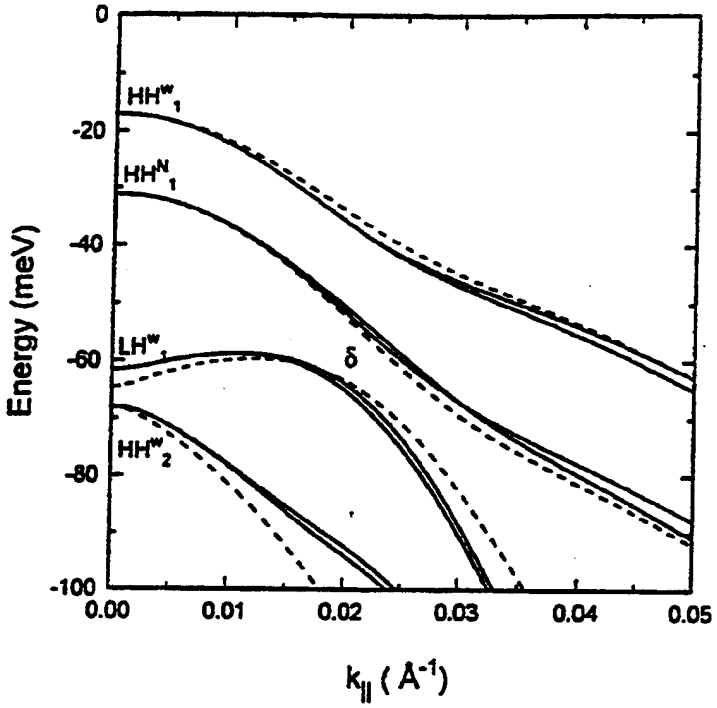

Figure 2. Valence band dispersion for the first four subbands of an asymmetric double quantum well structure

To supplement this research, our Cr:Forsterite pump/probe setup can excite and detect holes near the Gamma point in the narrow well. This excitation will prevent tunneling to the wide well, due to the lack of proximity to the mixed narrow and wide well bands. Thus, we expect to see only a slow component of hole relaxation, pertaining to hole decay to the Gamma point. We had expected to get the DQW sample in early January from Rich Leavitt at Adelphi, but he had several problems with his MBE machine. We expect to get this sample shortly in May, 1996 and will proceed thereafter with this measurement. This measurement is currently being conducted by Martin Jaspan, (JSEP supported) in collaboration with Rome Labs.

Additional research has been conducted by Eric Mozdy (Air Force Fellow) in conjunction with USAF Phillips Laboratory, Kirtland AFB, Albuquerque, NM. This work concerns controlling chaos, primarily the synchronization and control of chaotic oscillators. Mozdy spent the summer of 1994 in Albuquerque constructing chaotic oscillator arrays, then synchronizing each oscillator with unidirectional coupling, and finally controlling the entire array with occasional proportional feedback (OPF) [14]. The task of controlling

arrays of oscillators is entirely new, with applications in diode laser array stability, integrated circuit stability, and other varied array control applications. As David Cohen finished his dissertation at Cornell, Eric Mozdy assumed responsibility and stewardship of the modelocked NaCl APM laser.

Mozdy is also using the APM laser to observe chaotic behavior, in support of the work he did with Phillips Labs. Our experiments with chaos involve a NaCl color center additive-pulse mode locked (APM), shown below in Fig. 3. The main cavity embodies the "standard" linear configuration of a laser. This cavity is sync-pumped by a mode-locked Nd:YAG laser. The control cavity essentially consists of a 17 cm piece of single-mode, dispersion-shifted (D = 0 at 1.55 micrometer) optical fiber, and a retroreflector. This cavity is identical in length to the main cavity (whose length is identical to the Nd:YAG pump cavity).

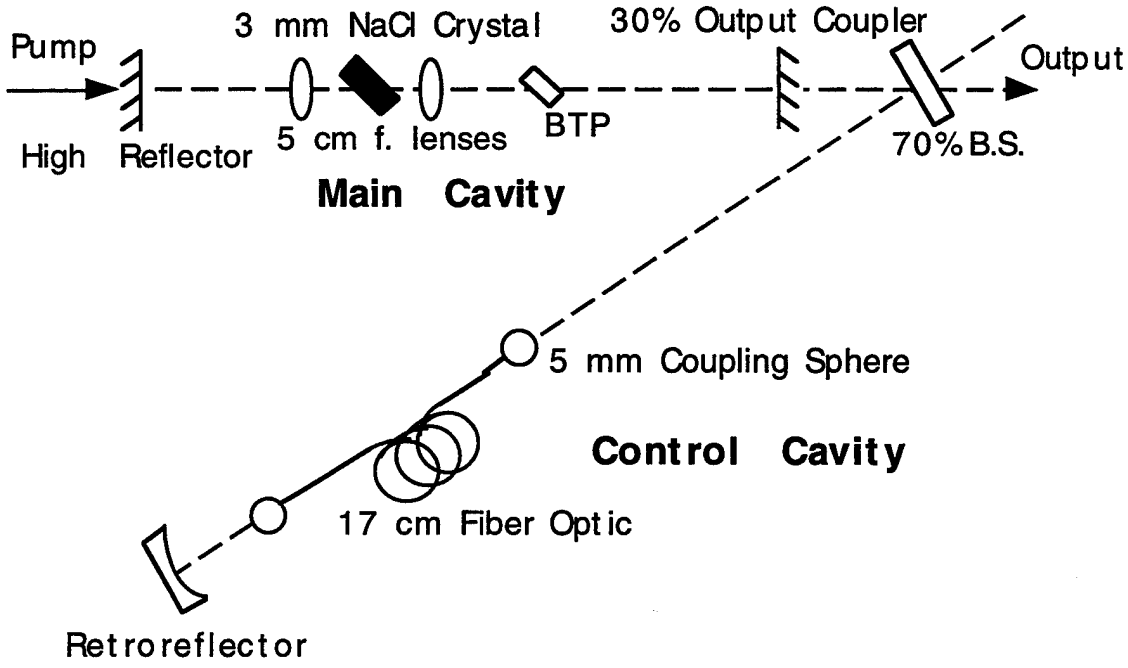

Fig. 3. Additive Pulse Modelocked Laser. The color center laser is coupled to a second cavity which contains a nonlinear optical fiber. The combination leads to ultrashort pulse generation.

The control cavity acts as a nonlinear output-coupler, because of self-phase modulation (SPM) within the fiber. This SPM phase-chirps pulses, which then recombine with those of the main cavity, causing destructive interference at the pulse wings, and constructive interference at the pulse peaks. Through this mechanism, the output coupler acts as a pulse-compressing nonlinear reflector. Empirically, the length of the fiber, the fiber coupling efficiency, the output coupler value, and the beamsplitter value all contribute in determining the final, steady state pulse width. With the values listed, we are producing about 150 fs pulses.

The fiber nonlinearity which sustains mode-locking is also the fundamental driving force behind chaos. Work in Chemla's group at Lawrence Berkeley Laboratory has demonstrated theoretically and experimentally that chaos should be significant in the APM laser. Moreover, their analysis predicts an entire period-doubling route to chaos, simply by increasing the amount of power in the fiber and hence, the amount of nonlinearity in the system. We have begun to experimentally explore the APM pulse-train bifurcations, which are indeed dependent upon fiber power. Already, we have demonstrated period one and two behavior, as well as quasiperiodicity. The periodic time series are shown in Figure 4 below.

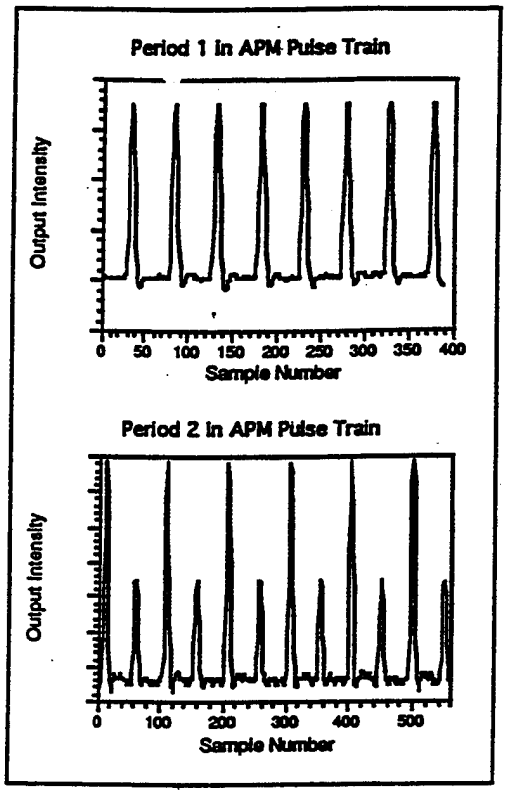

Fig.4. Data taken from an APM laser operating in period-1 and period-2 oscillations.

Currently, we are constructing a complete bifurcation diagram of the laser's period doubling behavior, and interacting with the Nonlinear Optics Group at the USAF Phillips Lab to fully characterize the chaotic behavior. Mozdy and Pollock travelled to Phillips Labs in Albuquerque in late March, 1996 to confer with Dr. V. Kovanis and Dr. A. Gavrielides. Time series data from our laser was transfered for analysis by the Phillips Lab team to characterize the degree of chaos-like behavior from the laser. We are in close contact with this group for theoretical direction of our experiments.

SCIENTIFIC IMPACT OF RESEARCH

Our measurements have served as the primary source for femtosecond carrier relaxation data in the self-consistent ensemble Monte Carlo based study of the carrier dynamics performed by the research group of Prof. Krusius. Only by comparison to solid measured data can the models and methods be established as being sound. We hope to gain insight into the hole dynamics of various structures. The ultimate goal of this work is to create optical devices, especially detectors, which operate at much faster speeds. The measurement of the impact of carrier and impurity scattering is essential to the development of better models and for better simulations.

DEGREES AWARDED

David Cohen, Ph.D., "Femtosecond Relaxation of Electrons in the Conduction Band of InGaAs," Ph.D. dissertation, Cornell University, 1995.

RELATED DEGREES AWARDED

Greg Williams, Ph.D., "Fabrication and Design Studies of Glass Based Waveguides and Electrooptic Devices," 1995.

REFERENCES

[1] G. Sucha, A.S.R Bolton, D.S. Chemla, D.I Sivco, and A.Y Cho, "Carrier relaxation in InGaAs heterostructures," *Applied Physics Letters*, 65, p. 1486-1488.

[2] Akihisa Tomita, Jagdeep Shah, J. E. Cunningham, Stephen M. Goodnick, P. Lugli, and Shun L. Chuang, "Femtosecond dynamics of non-thermal holes in n-modulation-doped quantum wells," *Semiconductor Science Technology* 9, pp. 449-452, 1994.

[3] Andrew Davidson, Richard Compton, Frank Wise, Dan Mars, Jeff Miller, "Femtosecond relaxation of minority electrons in heavily carbon-doped GaAs," *Journal of Applied Physics*, 76 p. 2255, 15 Aug 1994.

[4] David Cohen, "Femtosecond relaxation of electrons in the conduction band of InGaAs," PhD Thesis, Cornell University, 1995.

[5] E. Ott, C. Grebogi, and J. A. Yorke, "Controlling Chaos," *Phys. Rev. Lett.* p. 1196, 1990.

[6] W.L. Ditto, S.N. Rauseo, and M.L. Spano, "Experimental Control of Chaos," *Phys. Rev. Lett.* 65, 3211, 1990.

[7] E. R. Hunt, "Stabilizing High-period Orbits in a Chaotic System: the Diode Resonator," *Phys. Rev. Lett.* 67, 1953, 1991.

[8] R. Roy, T.W. Murphy, T.D. Maier, Z. Gills and E.R. Hunt, "Dynamical Control of a Chaotic Laser: Experimental Stabilization of a Globally Coupled System," *Phys. Rev. Lett.* 68, 1259, 1992.

[9] S. Bielawski, D. Derozier, and P. Glorieux, "Experimental characterization of unstable periodic orbits by controlling chaos," *Phys. Rev. A* 47, R2492, 1993.

[10] K. Pyragas, "Continuous control of chaos by self-controlling feedback," *Phys. Lett. A,* 170, 421, 1992.

[11] S. Bielawski, D. Derozier, and P. Glorieux, "Stabilization and characterization of unstable steady states in a laser," *Phys. Rev. A* 47, 3276, 1993.

[12] S. Bielawski, D. Derozier, and P. Glorieux, "Controlling unstable periodic orbits by a delayed continuous feedback," *Phys. Rev. E* 49, R971, 1994.

[13] J. Bair, D. Cohen, J. P. Krusius, and C. R. Pollock, "Femtosecond Relaxation of Carriers Generated by Near Band Gap Optical Excitation in Compound Semiconductors", Physical Review B 50, No. 7, 4355-4370, 1994.

[14] E. Mozdy, T. C. Newell, P. M. Alsing, V. Kovanis, and A. Gavrielides, "Synchronization and control in a unidirectional coupled array of chaotic diode resonators," Physical Review E, 51, 5371, 1995.

JSEP PUBLICATIONS

1. Alphan Sennaroglu, Clifford R. Pollock, and H. Nathel, "Efficient continuous-wave chromium-doped YAG laser," JOSA-B, 12, pp.930-937, 1995.

2. Mozdy, T. C. Newell, P. M. Alsing, V. Kovanis, and A. Gavrielides, "Synchronization and control in a unidirectionally coupled array of chaotic diode resonators," *Physical Review E*, 51, 5371, 1995.

JSEP RELATED PUBLICATIONS

1. R. P. Espindola, M. K. Udo, D. Y. Chu, S. L. Wu, S. T. Ho, R. C. Tiberio, P. F. Chapman, and D. Cohen, "All-optical switching with low-peak power in microfabricated AlGaAs waveguides,", *IEEE Photonics Technology Letters*, 7, 641, 1995.

OPTICAL PROCESSES AND CARRIER DYNAMICS IN ULTRAFAST COMPOUND SEMICONDUCTOR PHOTONIC DEVICES

Task #4

Task Principal Investigator: **J. Peter Krusius**
Office: (607) 255-3401
Lab: (607) 255-5034
Fax: (607) 254-4777
e-mail: krusius@ee.cornell.edu

OBJECTIVE

The objective of this task is to explore the physics and operation of ultra-high speed compound semiconductor based photonic structures and devices. The focus is on the interaction of optical processes and ultrafast carrier dynamics in both optical detector and source structures. The study is conducted theoretically via fundamental physics formulations and first principles device simulations in a close interaction with materials, optical measurement, and device fabrication tasks of this program. The goal in this task is to create understanding of the physics, design, measurements, and the ultimate limits of high speed photonic devices.

DISCUSSION OF STATE OF THE ART

Optoelectronic devices have been investigated for the past few decades. They are used in many applications including long distance communication and local area networks. The operation of such photonic systems places stringent requirements on the optoelectronic devices, including optical sources and amplifiers (light emitting diodes, semiconductor lasers) and photodetectors. Sources and amplifiers should have a high signal to noise ratio and a large modulation bandwidth for high speed applications. A high quantum efficiency is required to obtain sufficient light intensity, while electrical power requirements, and thermal stresses are kept low. Detectors should have both a high quantum efficiency and low noise to ensure that the minimum detectable power is sufficiently small for low level signals. For high speed communication a fast detector response time is necessary. Often devices should be small in size as well. This is important, for example, for optoelectronic devices which must have structures suitable for coupling into the transmission media, i.e. single or arrays optical fibers and waveguides. Analog applications require in addition that sources, amplifiers and detectors be sufficiently linear.

High quantum efficiency and low power dissipation in semiconductor lasers and light emitting diodes is determined by the confinement of carriers within the active region. Escaping carriers do not contribute to laser gain or the light generated by an LED. Confinement along the direction perpendicular to the optically active region can be realized by a number of schemes including homojunctions, heterojunctions and single, or multiple, quantum wells. Recently, quantum wire type two-dimensional confinement has been considered. Lateral current confinement has also been attempted through several techniques and is generally more difficult to achieve. Both LED's and semiconductor lasers suffer from quantum noise resulting from the statistical nature of carrier recombination. Lasers also exhibit modal noise, such as mode-partition noise in multimode lasers or jumping between modes in a single mode lasers. The modal noise can be reduced by limiting the lateral and transverse modes by optical confinement and by using wavelength dependent mirrors, such as Bragg reflectors to limit operation to a single longitudinal mode. The modulation bandwidth of an LED is determined primarily by the carrier recombination time in the active region, because their structure does not provide any transport mechanisms to sweep the carriers out of the active region. Thus, high speed modulation can only be achieved at the expense of high power operation. The modulation bandwidth in semiconductor lasers is ultimately limited by the relaxation oscillations of the laser field. This limits present laser modulation bandwidths to about 30 GHz, a rather low frequency compared to transistors.

In order to achieve the high quantum efficiency necessary to detect low level signals, current detectors require thick absorption regions. If not limited by extrinsic parasitic capacitances, the response time of a photodetector is ultimately determined by how rapidly the photogenerated electron-hole pairs can be separated and removed from the absorption region, either via transport or recombination processes. Thus in photodetectors, such as the PIN photodiodes, which employ a high electric field in the depletion region to separate carriers, there is a trade-off between sensitivity and speed. The fundamental causes of noise in photodetectors are shot noise due to the statistical nature of the absorption processes and the device dark current. Device responsivity can be increased through amplification processes, as in the avalanche photodiode, but only at the expense of increased noise.

State of the art optoelectronic sources and amplifiers incorporate a number of sophisticated structures including heterojunctions, quantum wells, and possibly quantum wires and dots in the near future, to provide simultaneous electrical and optical confinement. The physics of carrier transport in such structures is quite complex, and especially in the quantum structures, not fully understood. Further, the details of the inhomogeneous carrier distribution functions are important factors in laser performance. Hole burning in the carrier distribution functions and carrier heating have been shown to contribute nonlinear terms to the laser gain [1-2], while spatial hole

burning can contribute to laser instability [3]. The index of refraction, and the fundamental band gap are functions of the distribution of carriers both inside and outside the active region. This affects both the gain and the width of the laser line [4-6]. It has been found via the simulation of electronic devices that incorporate complex structures, such as heterojunctions and quantum wells, that such structures lead to the formation of space charge layers and large electric fields that have serious consequences for both the static and dynamic operation of the device [7]. These effects will also significantly influence all device characteristics from microscopic carrier distribution functions to macroscopic device parameters. Thus detailed information on the operation of photonic devices, should be derived from detailed first principles theoretical modeling combined with ultrafast optical measurements.

Many studies have been devoted to developing models for use in design and optimization of photonic semioconductor sources and detectors. However, in these studies the emphasis has been on the optical physics, while the complexities of carrier transport and device physics have been de-emphasized or even neglected. A variety of models of the behavior of semiconductor lasers can be found in the literature. These include models based on transmission lines [8-9], the circuit approach [10], coupled-wave theory [11], density matrix formulation [2,12] and rate equations [13-15]. In some of these models the optical aspects are quite sophisticated, but the rest of the device physics is highly simplified. In each of these cases the physics of the gain media is modeled by simple rate equations. Sometimes the active medium of the laser has been divided into a number of independent segments along the optical cavity. Each of these is then governed by an independent set of rate equations interacting only through the optical field. Therefore the details of the carrier transport, space charges, and distribution function effects are almost completely neglected. The most sophisticated models in the literature treat carrier transport within the drift-diffusion formalism in one or two dimensions [16]. However, drift-diffusion formulations are severely limited in their ability to account for the complex physics of non-equilibrium carrier transport, spatial inhomogeneities, quantum wells, the nonthermal carrier distributions resulting from hole burning, and other interactions between the carriers and optical field.

The modeling of optoelectronic detectors is somewhat better developed. Due to the simplicity of optical phenomena in these devices, considerably more care is often taken in the treatment of the device physics. Sophisticated transport techniques such as Monte Carlo simulation are even applied to such devices as metal-semiconductor-metal (MSM) photodetectors [17-19]. However in these cases, the simulations are usually simple applications of classical transport, often in simplified form, and do not include all the physical processes necessary to model these devices over a broad range of conditions. These cases include conditions of high optical excitation and carrier density, where carrier-carrier scattering, free carrier screening and band

renormalization are likely to play important roles. These phenomena have been shown to be significant primary effects in thin film structures probed by the femtosecond dual pulse correlation technique (this task). Past formulations do not account for the use of heterostructures increasingly seen in detectors fabricated in small band gap materials [20-21]. Also, in contrast to laser models the optical physics is frequently modeled very crudely, often just assuming a priori the functional form of the optical excitation.

The ability to accurately describe all significant aspects of the physics of optoelectronic devices is severely limited in published models. In order to understand the principles of operation and design of the highest speed photonic devices it will necessary to simultaneously examine both the optical and electronic aspects of these devices using sophisticated models and simulations that account for all of the complex physical processes on a level comparable to that used in our femtosecond dual pulse correlation formulation. Such a first principles approach will also provide information on the fundamental limits and the ultimate achievable speeds. Finally, practical device design trade-offs for this class of photonic devices will then be well understood.

PROGRESS

Our research on the microscopic physics of femtosecond tunable dual pulse correlation probing of narrow band gap semiconductors has been taken to a virtual end. Careful correlations between the theory done in this task and experiments performed in Pollock's group mandated the inclusion of many physical processes that are outside the traditional Monte Carlo method. These include Coulomb enhancement, band renormalization, and free carrier screening, all of which arise from the breakdown of the semi-classical and single particle approximations. These two approximations forms the foundation for the traditional approach to describing the dynamics of carriers in semiconductors. Once these processes were included, the resulting Monte Carlo formulation was applied to the study of optically generated carrier relaxation on the time scale from 100 fs to about 2 ps in the near band gap regime that was accessible to the available tunable femtosecond laser probe. The 100 fs lower bound is determined by the coherent artifact, a characteritic of the dual pulse correlation technique. The simulations reproduced and explained the measured data on a quantitative level without any adjustable parameters, a truly remarkable achievement. Essentially all features in the data measured for intrinsic samples were explained. The observed relaxation can be described by the thermalization of the electron distribution. Band renormalization and Coulomb enhancement were found to set the initial conditions for the thermalization and determine the relationship between the transmission of the optical probe pulse and the evolution of the carrier

distribution functions. The thermalization was found to be rather insensitive to most carrier scattering processes.

The application of this methodology to heavily doped n-type samples was not as successful, although a qualitative understanding was reached. Beyond the coherent artifact, a characteristic of all dual pulse correlation measurements, or beyond about 300 fs for doped samples, the observations could be explained with the thermalization of the perturbed electron distribution with the lattice, as was done for unpoded samples. However, the initial carrier-carrier mediated relaxation occurred much faster and the polar optical phonon mediated relation much slower than in undoped samples. The background electron plasma thus enhanced electron-electron scattering, while blocking phonon scattering. Inside the coherent artifact the initial excited carrier distribution is likely to be changed in a way not accounted for by our methodology. This observation may be an expression of the fact that our methodology is reaching its fundamental limitations under these extreme non-equilibrium conditions.

This fundamental physics based methodology has now been fully extended to the study of optical detectors. New physical processes that were added include the provision for inhomogeneous doping and improvements in the treatment of very short length scale variations in the carrier density, the extension of the previous treatment of the interaction with the optical field to include spontaneous emission (radiative recombination), the description of metal-semiconductor contacts using first principle carrier dynamics, and the extension of the model band structure to describe the conduction band L valley minima. A complete optoelectronic device simulator package OPTMC has been written, debugged, tested and verified. OPTMC describes the optical field, the interaction between photons and electrons and holes, and dual carrier relaxtion and transport processes. Spatial variables for photons, electrons and holes are described in one dimensions and momentum space variables in three dimensions.

An extensive study of the response of metal-semiconductor-metal (MSM) photodiodes has been conducted using OPTMC. It was found that the intrinsic impulse response of the photodetector has three components (Fig. 1). First, the device current shows an initial fast response on the order of few picoseconds depending on device design that is due to velocity overshoot of photogenerated electrons in the Γ valley. The slow secondary response is determined by electrons being swept out of the device at lower steady state drift velocities. The final third response comes from the slow hole drift processes occurring at the much lower steady state hole drift velocities. However, each of these components is a complex function of the local electric fields and the device structure, and therefore the overall device response is quite complex. The effect of the exciting photon energy on the two electron responses is another significant factor. Excitations high above the band edge

allowed a lot of electron transfer into the L valley and hence had a large detrimental effect on the transient overshoot amplitude and electron transit time. Screening of the electric field by the excited carriers was observed at high excitation levels. Under some conditions we observed plasma oscillations, however these would have little consequence for normal photodetector operation. The slow hole response can be improved by special device designs but only at the expense of the electron response. These issues are being explored further in an interaction with Compton's group.

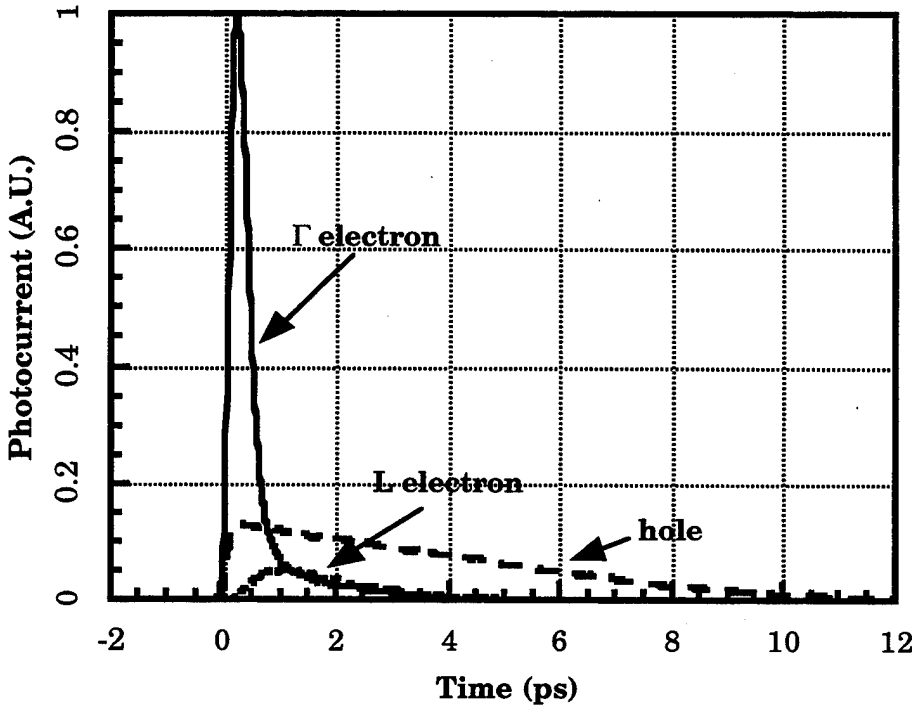

Fig. 1 Impulse response of GaAs MSM photodiode in terms of its normalized photocurrent as a function of time. The length of the device is 0.5 μm and the applied field 20 kV/cm. The width of the optical pulse is 100 fs (FWHM). Simulations were performed with about 50, 000 electrons and a time step of about 10 fs.

We have also examined the photodetector response under conditions where a pulse train with equidistant spacing excites the photodiode. If the spacing between the pulses is shorter than the device response time, there will be a residual carrier population, when the next pulse enters the device. Because of the impact on screening associated with this residual background, nonlinear phenomena may occur that are not present in the impulse response. One such example is the observation of optically pumped current oscillations (Fig. 2), which occurred with a pulse spacing of 1 ps or a frequency of 1 THz! The amplitude of these oscillations was as large as the impulse response, i.e. 100%. This is the first time such oscillations have been observed.

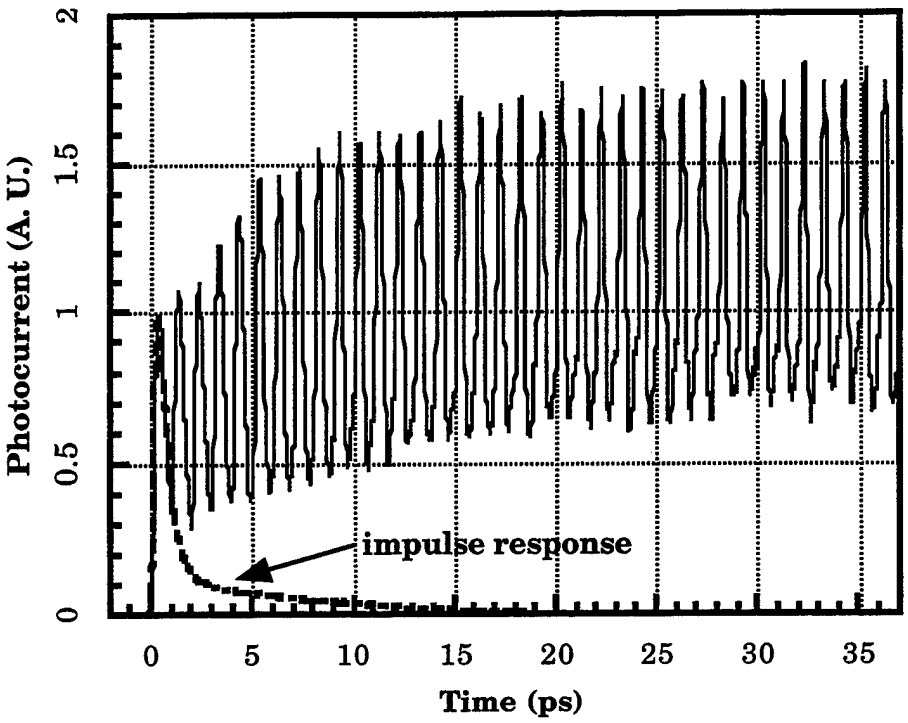

Fig. 2 Response of optically pumped MSM oscillator in terms of its normalized photocurrent as a function of time. The length of the device is 0.5 μm and the applied field 10 kV/cm. The width of the optical pulse is 100 fs (FWHM) and their spacing is 1 ps. Each optical pulse generates about $1x10^{16}$ cm^{-3} electron-hole pair. The impulse response for a single pulse is shown as well.

SCIENTIFIC IMPACT

The self-consistent emsemble Monte Carlo methodology developed in this work has virtually been taken to the end in the analysis of current femtosecond dual pulse correlation measurement technique performed by Pollock's group on near band gap carrier relaxation. Agrrement between theory and experiment has been remarkable. This methodology has been extended to optoelectronic devices and shown to provide a truly fundamental foundation for investigating their microscopic physics. At the current level it facilitates the investigation of the behavior of semiconductor photodetectors on a more fundamental level than has ever been attempted. The results have not only improved the understanding of known phenomena in complex device environments, but also provide an opportunity to study new phenomena and concepts that have not been reported due to the inadequacy of previous device physics. The timescale of basic processes, such as carrier-carrier and photon-carrier interactions, has now been bridged all the way to the complete switching response of the device. The fundamental microscopic limits of the switching of metal-

semiconductor-metal photodetectors have already been quantified. Based on this new photodetectors designs have been considered with Compton's group. We will proceed in further collaborations with Y.H. Lo's group towards the study of the fundamental physics of optical sources.

DEGREES AWARDED

James E. Bair, "Monte Carlo Simulation of Ultrafast Carrier Dynamics and Optical Interactions in Compound Semiconductor Thin Films and Optical Devices," Cornell University PhD Thesis, pp. 1-359, August 1995.

REFERENCES

[1] "Origin of Nonlinear Gain Saturation in Index-Guided Laser Diodes", R. Frankenberger and R. Schimpe, Appl. Phys. Lett., 60, 22, 2720 (1992).

[2] "The Gain and Carrier Density in Semiconductor Lasers Under Steady-State and Transient Conditions", B. Zhao, T. R. Chen, and A. Yariv, IEEE J. Quant. Elec., 28, 6, 1479 (1992).

[3] "Longitudinal Spatial Instability in Symmetric Semiconductor Lasers due to Spatial Hole Burning", R. Shatz, IEEE J. Quant. Elec., 28, 6, 1443 9 (1992).

[4] "Band Gap Shrinkage in GaInAs/GaInAsP/InP Multi-Quantum Well Lasers", S. H. Park, J. I. Shim, K. Kudo, M. Asada, and S. Arai, J. Appl. Phys., 72, 1, 279 (1992).

[5] "Effect of Free Carriers on the Linewidth Enhancement Factor of InGaAs/InP (strain layered) Multiple Quantum Well Lasers", L. F. Tiemeijer, P. J. Thijs, J. J. M. Binsma, and T. V. Dongen, Appl. Phys. Lett., 60, 20, 2466 (1992).

[6] "Carrier-Induced Change in Index, Gain, and Lifetime for $(InAs)_1/(GaAs)_4$ Superlattice Lasers", N. K. Dutta, N. Chand, and J. Lopata, Appl. Phys. Lett., 61, 1, 7, (1992).

[7] "Heterojunction Vertical FET's Revisited: Potential for 225 GHz Large Current Operation", S. Weinzierl and J.P. Krusius, IEEE Transactions on Electron Devices, 39, #5, 1050-1055 (1992).

[8] "New Dynamic Model for Multimode Chirp in DFB Semiconductor Lasers", A. J. Lowery, IEE Proc., J137, 5, 293 (1990).

[9] "Modelling Spectral Effects of Dynamic Saturation in Semiconductor Laser Amplifiers Using the Transmission-Line Laser Model", A. J. Lowery, IEE Proc., J136, 6, 320 (1989).

[10] "Circuit Theory of Laser Diode Modulation and Noise", J. Arnoud, M. Esteban, IEE Proc., J137, 1, 55 (1990).

[11] "Two-Dimensional Theory of Distributed Feedback Semiconductor Lasers", H. Sato, and Y. Hori, IEEE J. Quant. Elec., 26, 3, 467 (1990).

[12] "Theory of Hot Carrier Effects on Nonlinear Gain in GaAs-GaAlAs Lasers and Amplifiers", B. N. Gomatam and A. P. DeFonzo, 26, 10, 1689 (1990).

[13] "Chaos in Semiconductor Lasers with Optical Feedback: Theory and Experiment", J. Mork, B. and Tromborg, J. Mark, IEEE J. Quant. Elec., 28, 1, 93 (1992).

[14] "Dynamic Detuning in Actively Mode-Locked Semiconductor Lasers", P. A, Morton, R. J. Helkey, and J. E. Bowers, IEEE J. Quant. Elec., 25, 12, 2621 (1989).

[15] "The Effect of Electronic Feedback on Semiconductor Lasers", K. and M. M. Ibrahim, IEEE J. of Quantum Elec, 26, 8, 1347 (1990).

[16] "A Self-Consistent Two-Dimensional Model of Quantum-Well Semiconductor Lasers: Optimization of a GRIN-SCH SQW Laser Structure", IEEE J. of Quantum Elec., 28, 4, 792 (1992).

[17] "Picosecond electron and hole transport in metal-semiconductor-metal photodetectors", J. Kuhl, M. Klingenstein, J. Rosenweig, C. Moglestue, and A. Axmann, Semicond. Sci. Technol., 7, B157 (1992).

[18] "Subpicosecond characterization of carrier transport in GaAs-metal-semiconductor-metal photodiodes", M. Lambsdorff, M. Klingenstien, and J. Kuhl, Appl. Phys. Lett., 58, 13, 1410 (1991).

[19] "Nanoscale Tera-Hertz Metal-Semiconductor-Metal Photodetectors", Stephen Y. Chou and Mark Y. Liu, IEEE J. Quantum Elec., 28,19, 2358 (1992).

[20] "Very high speed GaInAs metal-semiconductor-metal photodiode incorporating an AlInAs/GaInAs graded superlattice", O. Wada, H. Nobuhara, H. Hamaguchi, T. Mikawa, A. Tackeuchi, and T. Fujii, Appl. Phys. Lett., 54, 1, 16 (1989).

[21] "High-Performance Undoped InP/n--$In_{0.53}Ga_{0.47}As$ MSM Photodetectors Grown by LP-MOVPE", Chang-Xin Shi, Detlev Grutzmacher, Manfred Stollenwer, Qing-Kang Wang, and Klaus Heime, IEEE Trans. Elec. Dev., 39, 5 1028 (1992).

JSEP PUBLICATIONS

1. J.E. Bair and J.P. Krusius, "Monte Carlo Simulation of the Fundamental Photodetector Response on Sub-Picosecond Time Scales", presentation Proceedings of IEEE/Cornell Conference on Advanced Concepts in High Speed Semiconductor Devices and Circuits, IEEE, 95CH35735, pp. 93 - 102, 1995

2. J.E. Bair and J.P. Krusius, "Impact of Dynamic Screening and Carrier-Carrier Scattering on Non-Equilibrium Dual Carrier Plasmas", Hot Carriers in Semiconductors Conference, edited by K. Hess, JP. Leburton, and U. Ravaioli, Plenum Press, pp. X - Y, 1995.

JSEP PUBLICATIONS IN PROGRESS

1. J.E. Bair and J.P. Krusius, "Microscopic View of Principles of Operation of Ultra-Fast MSM Photodetetors", manuscript in preparation for IEEE J. Lightwave Technology, to be submitted for publication in August 1996.

2. J.E. Bair and J.P. Krusius, "Impact of Dynamic Screening and Carrier-Carrier Scattering on Carrier Relaxation and transport in Dense Dual Carrier Plasmas", manuscript in preparation for Journal of Applied Physics, to be submitted for publication in October 1996.

3. J.E. Bair and J.P. Krusius, "Effect of Photon Energy and Pulse Intensity on the Observed Relaxation of Carriers Excited Near the Band Gap in III-V Semiconductors", manuscript in preparation for Physical Review, to be submitted for publication in December 1996.

RELATED PUBLICATIONS

1. J. Sutherland., G. George and J.P. Krusius, "Alignment Tolerance Measurements and Optical Coupling Modeling for Optoelectronic Array Interfaces", Proceedings of the 46th Electronic Components and Technology Conference, IEEE 96CH35931, pp. 480 - 486, 1996.

ULTRA FAST STRAIN-COMPENSATED MULTIPLE QUANTUM WELL LASERS

Task #5

Task Principal Investigator: **Yu-Hwa Lo**
Office: (607) 255-5077
Fax: (607) 254-4565
e-mail: yhlo@ ee.cornell.edu

OBJECTIVE

The objectives of this task are (1) to explore innovative device and material structures for ultra fast long wavelength (1.3/1.55 micron) semiconductor lasers and (2) to demonstrate the unique advantages of strain-compensated quantum wells in long wavelength vertical surface emitting lasers (VCSELs). This task is closely linked to Task 1 (Shealy) which provides strain compensated superlattice and quantum wells for our device study. Our research will also benefit significantly from the fundamental physics studies on carrier relaxation and transport performed in Task 3 (Pollock) and Task 4 (Krusius).

DISCUSSION OF STATE-OF-THE-ART

From a practical point of view, all lightwave systems prefer to use optical sources with a surface emitting, circular beam profile, as opposed to devices with an edge emitting, elliptical beam profile. Vertical cavity surface emitting laser (VCSEL) is an ideal choice because it has these desired beam properties. In addition, VCSEL possesses many unique attractive characteristics vital to high-speed data transmission. For example, it operates at a single wavelength with a side mode suppression ratio of greater than 30 dB, comparable to the value of costly DFB and DFB lasers. Single mode operation is important for high-speed communication since it reduces signal dispersion and mode partition noise by orders of magnitude. VCSELs can also be easily integrated into arrays with minimum extra fabrication and packaging efforts [1,2]. For advanced wavelength division multiplexing (WDM) systems, VCSEL is the most promising cost-effective approach for WDM laser arrays [3].

The first technology breakthrough on VCSELs occurred about seven years ago when Jewell et al, then at AT&T Bell Labs., reported the first low threshold current GaAs VCSEL at 980 nm wavelength using GaAs/AlAs Bragg mirrors and InGaAs/GaAs strained quantum wells [1]. Shortly after this breakthrough, world-wide research activities have been stimulated and progress has been made in an ever faster speed [2-5]. A few months ago, threshold current for GaAs VCSELs has been reduced from more than 1 mA

to around 100 μA [5-7], with an astonishing record of 9 μA threshold reported by a research group from USC [8]. Using the similar design of 830nm and 980 nm VCSELs, VCSELs operating in the visible regime around 670 nm [9,10] have also been demonstrated with impressive performance. This progress is significant for low cost optical communication since 670 nm light has low loss in plastic fiber. In the meanwhile, GaAs VCSELs have been moved quickly from research laboratories to market place, and many companies including Motorola and Hewlett Packard have announced or scheduled their products. In contrast with the rapid advances of GaAs-based VCSELs, relatively slow progress has been made on InP-based 1.3 and 1.55 micron wavelength VCSELs in spite of their undoubted significance for optical communication. The disparity of the progress between GaAs and InP VCSELs is attributed to many reasons, of which some are inherent and others are more material and technology related. Those inherent reasons, including Auger recombination, intervalence band absorption, and diffraction loss, are associated with the longer wavelength or lower photon energy. Those material and technology related reasons include low reflectivity of InP/InGaAsP Bragg mirrors, high series resistance, and low thermal conductance of InGaAsP epilayers and InP substrate. As a result, all the 1.3 and 1.55 micron VCSELs except few still operate in a pulsed condition at room temperature, and their pulsed threshold currents are orders of magnitude higher than their GaAs counterpart.

It was finally realized that the same design principle that has resulted in great success for GaAs-based VCSELs can not be directly applied to long wavelength VCSELs. It calls for innovative designs to cope with the unique set of problems for long wavelength VCSELs. Recently, two important innovative technologies were proposed and demonstrated by our group at Cornell and almost simultaneously, a research group from UC Santa Barbara. These two inventions are the use of strain-compensated multiple quantum wells (SC-MQWs) and bonded (fused) mirrors [11-15]. After applying both techniques to long wavelength VCSELs, the pulsed threshold current of 1.55 μm VCSEL has been reduced by nearly one order of magnitude to around 10 mA; and subsequently, the UCSB/HP research group demonstrated the world first 1.55 μm room temperature, cw operating VCSEL [15].

Because of the drastic performance improvement, we have the opportunity, for the first time, to study the dynamic spectral response of 1.55 micron VCSELs and compare the data with those achieved from conventional DFB lasers [16]. Our current JSEP program is playing a key role for this accomplishment since we started our investigation of strain-compensated quantum wells in this program.

PROGRESS

1. 1.5 μm Vertical-Cavity Surface-Emitting Lasers with Strain-Compensated Multiple Quantum Wells (SC-MQWs)

We investigated a promising laser structure, strain-compensated multiple-quantum-well (SC-MQW) vertical-cavity laser for optical communication. Strain compensation is achieved by growing quantum wells and barriers with opposite strain (e.g. compressive wells and tensile barriers or vice versa). To balance the strain over a large number of quantum wells, the material growth is very challenging. Working closely with Professor Shealy (Task 1) and industrial collaborators (Bellcore, ATT Bell Labs., and Sandia National Labs.), we obtained strain-compensated multiple quantum wells using OMCVD technique. The residue strain in the samples is within 0.1%, measured by x-ray diffraction.

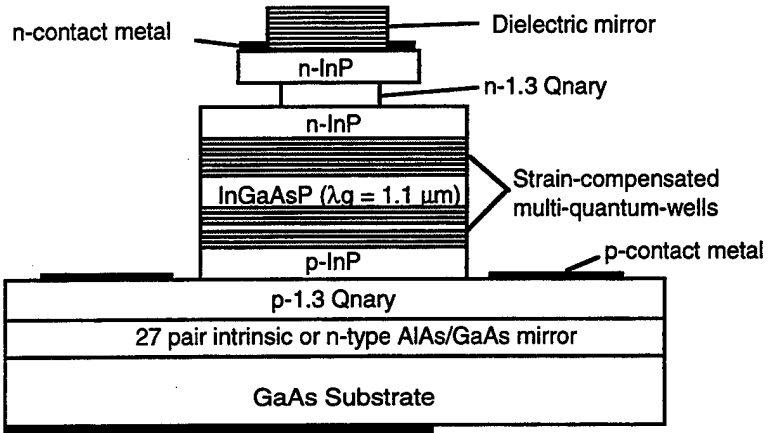

Fig. 1 Schematic of VCSEL using strain-compensated quantum wells and GaAs/AlAs bonded back mirror.

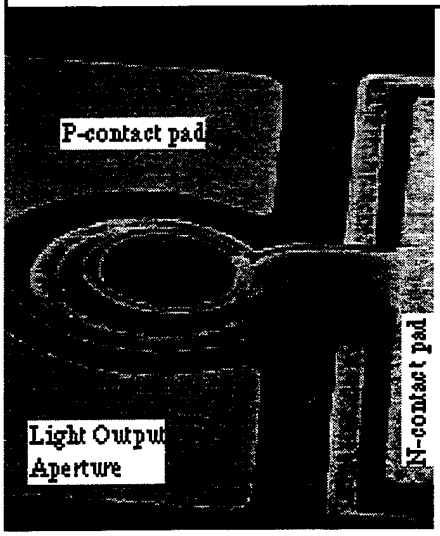

Fig. 2 SEM photograph of a 1.5 μm VCSEL with dielectric/ metal composited mirror bonded to a Si substrate.

In addition to the SC-MQW structure, we also developed a new mirror forming technology using wafer bonding technique. This new technology allows us to transfer the strain-compensated quantum wells from their native InP substrate to a new substrate. Many advantages are expected out of this wafer bonding process: First, we can fabricate long wavelength VCSELs to substrates such as Si and AlN which have a much higher thermal conductance than InP. Second, we can use new mirror structures that are impossible to fabricate directly on InP. Figure 1 shows the schematic of a VCSEL using GaAs/AlAs Bragg mirror, and Figure 2 shows the SEM photograph of a VCSEL having dielectric/metal mirror on a Si substrate. Both device structures have threshold currents of 10 mA to 16 mA in room temperature, pulsed condition (Fig. 3). This was among the lowest threshold currents for 1.55 micron VCSELs reported to date. The device operates at a single longitudinal and spatial mode up to three times of the threshold current, demonstrating its potential as a DFB like single frequency laser. The bonding process seems to have a good yield and uniformity (Fig. 4). The remaining problems to be solved in order to achieve cw operation (the main objective for our next JSEP program) are reducing ohmic heating and improving carrier confinement.

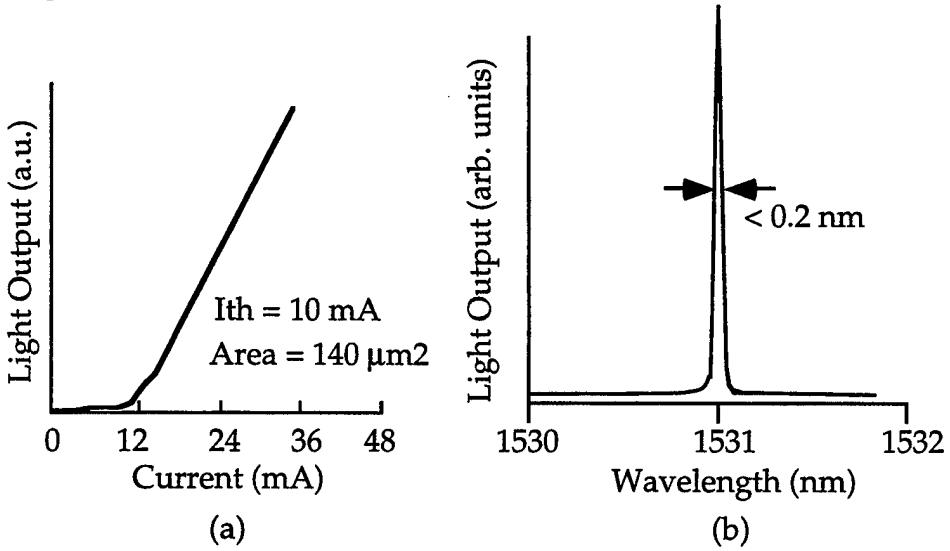

Fig. 3 Pulsed L-I characteristics (a) and optical spectrum (b) of a VCSEL operating at room temperature.

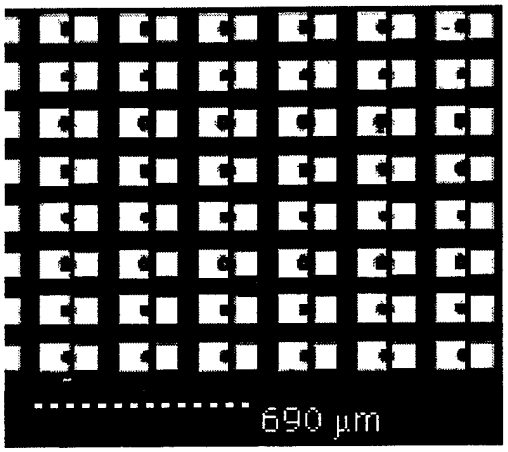

Fig. 4 Optical microscope photograph of an array of 1.55 µm VCSELs with a wafer bonded GaAs/AlAs Bragg mirror.

2. *Physics for Ultra-High-Speed Semiconductor Lasers*

Tremendous efforts have been taken over the last a few years to optimize the high-speed performance of qnautum well lasers. Recently, QW lasers with a modulation bandwidth of over 30 GHz have been demonstrated. However, many military and commercial applications such as phase array antenna and fiber optic RF signal transmission requires 40 GHz or higher bandwidth. Hence it is important to find out the major limitations on the modulation bandwidth of QW lasers. Our investigation found that spectral hole burning, carrier heating, and carrier transport are the most critical bandwidth limiting processes. These processes can be further characterized by a number of time constants including carrier dephasing time, carrier energy relaxation time, and carrier diffusion-capture-escape times.

To investigate the effects of spectral hole burning, carrier heating, and carrier transport on the modulation bandwidth of QW lasers, we have developed a comprehensive model that includes the following features:

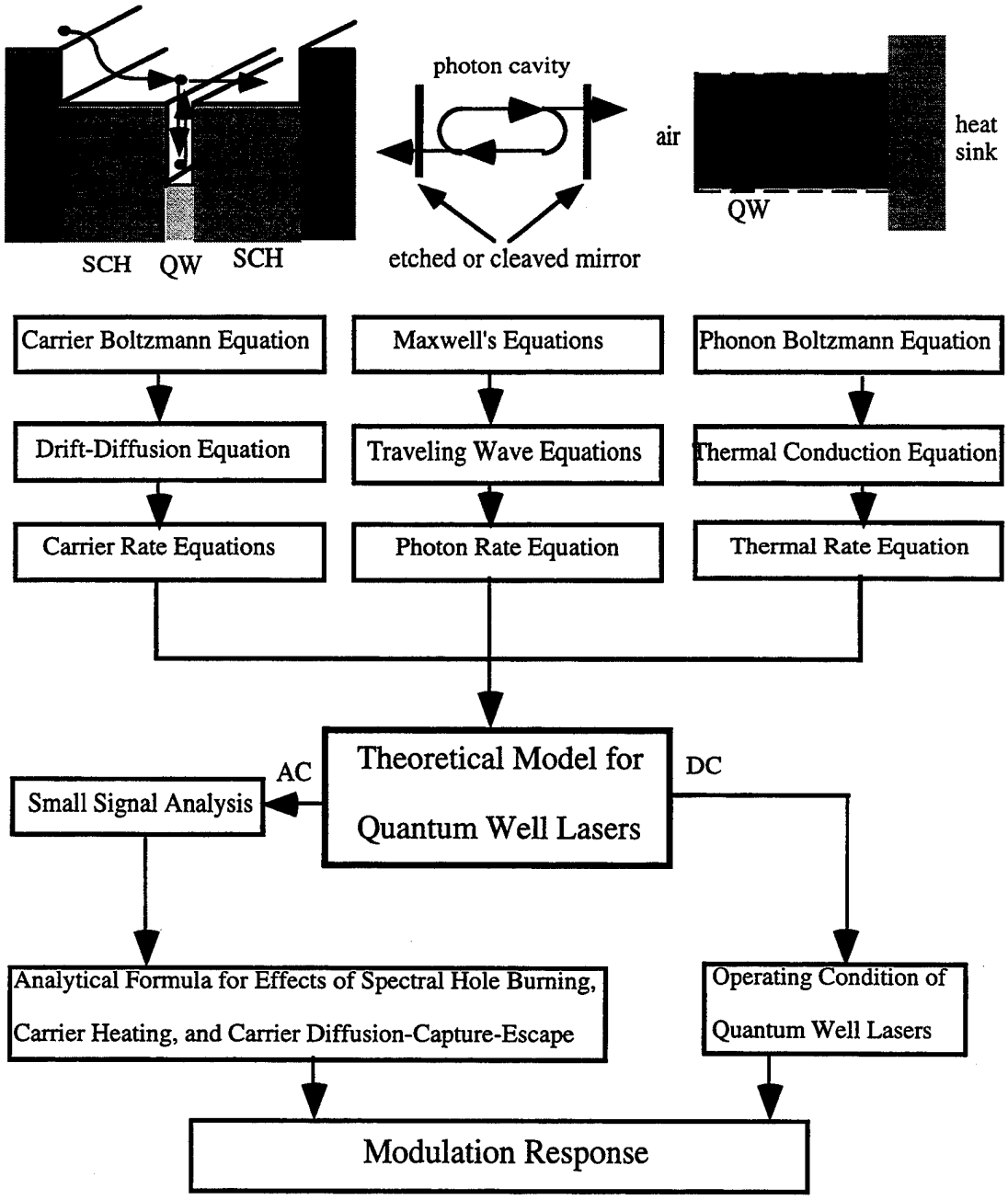

Figure 5. Schematic diagram of the theoretical frame for quantum well lasers.

(1) To accurately describe the interaction between carriers, photons, and phonons in the QW lasers, we derived a set of rate equations in our theoretical model from the carrier Boltzmann equation, Maxwell's equation, and phonon Boltzmann equation and thus eliminate any errors associated with the phenomenological models (Fig. 5).

(2) To make our theoretical model more realistic and accurate, we calculated the carrier dephasing time, carrier energy relaxation time, and

carrier quantum capture and escape times from first principles instead of assigning arbitrary time constants as done in conventional approaches.

(3) Since these three physical processes mutually influence each other, we simultaneously consider their effects on the small-signal modulation response of QW lasers, instead of separately focusing on one or two of these physical processes as the conventional approach does.

(4) From our theoretical model, we numerically determine the temperatures of electrons, holes, and lattice in the operating condition of QW lasers. We also can simulate the population distribution of longitudinal optical (LO) phonons by incorporating the hot phonon effect in QW lasers (Fig. 6).

(5) To investigate the effects of these physical processes on the small-signal modulation response of the QW lasers, we perform an elaborate small signal analysis on our rate equations and obtain an exact analytical solution for the modulation response of QW lasers. From our exact small signal analysis, the nonlinear gain coefficients associated with the effects of spectral hole burning, carrier heating, and carrier transport are thus unambiguously defined. Their relations with the modulation bandwidth of QW lasers are rigorously derived.

Several interesting results are obtained from our theoretical model:

(1) Carrier capture and escape times in an AC condition are significantly different from those obtained in a DC condition. Our results indicate that the conventional models that do not distinguish the differences between the DC and AC capture and escape times may underestimate the influence of carrier transport on the modulation bandwidth of QW lasers.

(2) Our first-principle calculations show that the DC escape time predicted by the classical thermionic emission theory is no longer valid if the width or depth of the QW is small. Therefore, in that case, the first principle calculation is indispensable for estimating the carrier escape time in QW lasers.

(3) Contrary to conventional belief, our small-signal analysis shows that the nonlinear gain coefficient due to free carrier absorption affects only the damping rate of the modulation response of semiconductor lasers but not the resonant frequency.

(4) Since it takes about 3 ps for LO phonons to decay into acoustic phonons at room temperature, this will cause the hot phonon effects on the carrier energy relaxation processes. Our theoretical calculations indicate that neglecting these hot phonon effects will underestimate the carrier energy relaxation time by almost an order of magnitude and thus severely underestimate the effects of carrier heating on QW lasers. Therefore, it is very crucial to take into account the hot phonon effect when modeling carrier heating of QW lasers.

(5) As the carrier temperature increases due to the effects of carrier and lattice heating, more carriers will escape from the QW and fewer carriers will be captured into the QW. At high bias current levels, this mechanism will

severely degrade the resonant frequency, significantly increase the nonlinear gain coefficient due to carrier transport (Fig. 7), and thus ultimately limit the modulation bandwidth of QW lasers.

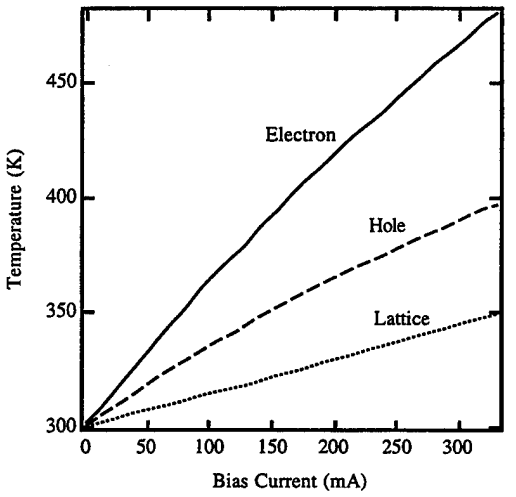

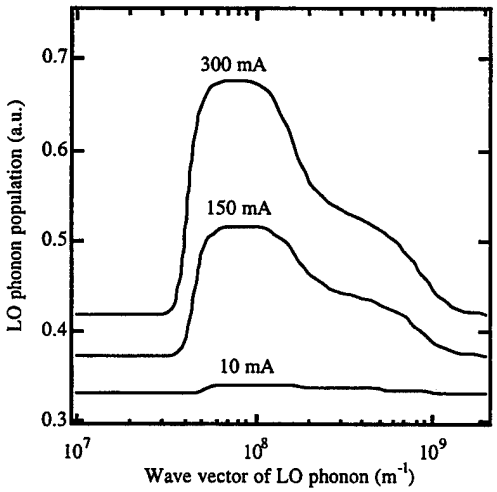

(a) (b)

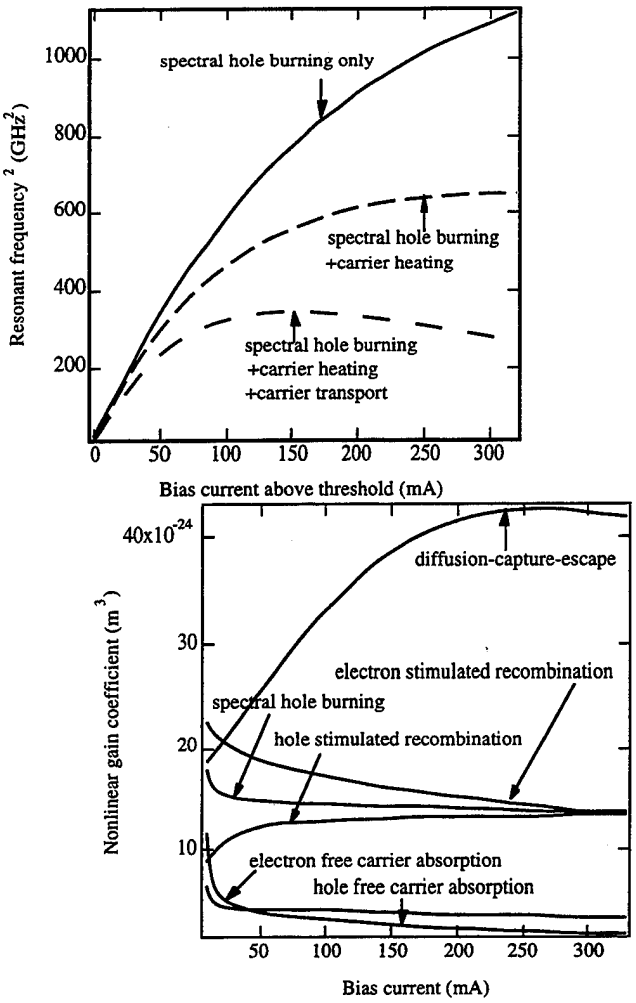

Fig. 6 (a) Electron temperature, hole temperature, and lattice temperature as a function of the bias current in a 50Å $Al_{0.3}Ga_{0.7}As/GaAs$ SCH single QW laser. The width of the SCH is 1000Å. The length between the QW and the heat sink is 100μm. (b) Population distribution of LO phonons as a function of LO phonon wave vector at different bias currents. (c) Square of the resonant frequency vs the bias current above threshold. (d) Nonlinear gain coefficients due to the effects of carrier diffusion-capture-escape, spectral hole burning, stimulated recombination heating, and free carrier absorption heating.

From our theoretical study, we thus identify the enhancement of carrier escape (overflow) processes due to the effects of carrier and lattice heating is the major physical mechanism that limits the modulation bandwidth of QW lasers; therefore, it is very crucial to reduce the magnitude of carrier or lattice heating if we want to improve the modulation bandwidth of QW lasers. To reduce lattice heating, we can flip-chip bond the laser diode to a good thermal conductor such as diamond or AlN. The most effective approach will be using the epitaxial bonding technique as described earlier to fabricate lasers directly on the heat conducting substrate. This will shorten the path of thermal conduction from the QW to the heat sink by more than an order of

magnitude. Our theoretical results also indicate that using p-doping in the active region of QW lasers will provide an additional channel for electrons to relax their energy to holes by electron-hole scattering and may reduce the electron temperature. However, the possible side effect of increasing intervalence band aborption due to p-doping has to be examined.

We have focused most of our theoretical effort in studying the small-signal amplitude modulation (AM) response of QW lasers (i.e., in the frequency domain). It will be straightforward to use our theoretical model to analyze other modulation schemes, such as FM, PM, ASK, FSK, and PSK and the large-signal behaviors. Issues like chirping and intermodulation distortion can thus be more detailedly characterized. Moreover, our theoretical model can also be implemented to investigate the effects of spectral hole burning, carrier heating, and carrier transport in the gain switched or mode-locked quantum well lasers (i.e., in the time domain). Incorporating the noise model into our theoretical frame, we hope that our comprehensive theoretical model can detailedly predict the overall dynamic behavior of semiconductor QW lasers.

3. Nonuniform Pumping for Strain-Compensated MQW Lasers

Beacsue a greater than usual optical gain is needed to compensate for the loss, long wavelength VCSELs normally contain a larger number of strain-compensated quantum wells. However, the gain a structure can produce at a given injected current could be much lower than the predicted value because of carrier transport limit. Carrier transport not only affects the dynamic response of a laser diode as discussed in the previous section, it also influences its static characteristics such as threshold current. This is particularly important for long wavelength VCSELs because high gain at low current injection is the key to achieve room temperature, cw operation. Under DC condition, the most prominent effect of carrier transport is nonuniform quantum well pumping. Since electrons and holes are injected from two different sides of the p/n junction and they have to overcome many potential barriers to reach the other end, each well may have a different carrier population, so called nonuniform pumping. When nonuniform pumping occurs, those heavily populated wells experience gain saturation and higher Auger recombination, and those under populated wells provide low optical gain. To realize the maximum advantages of multiple quantum well structures in long wavelength VCSELs, we have to understand nonuniform pumping and develop schemes to minimize it.

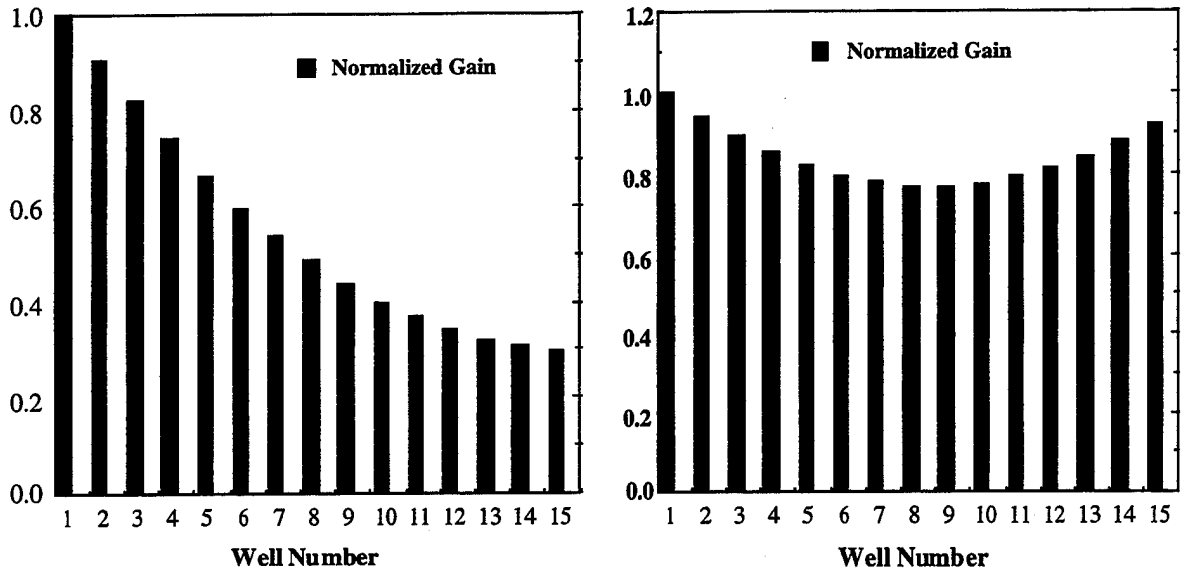

(a) (b)

Fig. 7 Normalized optical gain distribution among the quantum wells due to nonuniform carrier injection (pumping). Nonuniform pumping effect is much more serious for undoped quantum wells (a) than for quantum wells with an exponential p-doping profile (b).

Our analysis was based on the assumption that holes are the bottleneck for carrier transport because of their low mobility. This assumption is still valid even when the concept of mobility can not be applied because the transport of heavy holes in the surface normal direction is much more difficult than electrons. Based on our previous studies on quantum capture and escape processes and carrier-phonon scattering, we incorporated these quantum transport effects into the rate equations of strain-compensated MQW lasers to study the nonuniform pumping effect. Foe each quantum well, we had one equation for the 2D (confined) electrons and one for the 2D (confined) holes. This yielded 2N coupled, nonlinear differential equations for a structure with N quantum wells. In addition, we had one equation for photons and one for 3D holes to describe the carrier motion in the unconfined states. In spite of the very involved mathematics, we solved the problem numerically and drew important conclusions. Figure 7(a) shows the effect of nonuniform pumping for 15 strain-compensated quantum wells. Clearly, those wells close to the p-side receive much more carriers and have a much higher gain than those away from the p-side, which manifests the effect of nonuniform pumping. To alleviate this problem, we propose to introduce a p-doping profile during material growth that can compensate for the decreasing hole population. Assisted with numerical analysis and physical insight, we found that the most effective p-doping profile had an exponential function with a characteristic length of the order of the diffusion length of holes in the separate confinement and barrier region. Figure 7(b) shows the improvement

achieved with such a p-type doping profile. After carrying out further calculations, we found that a 50% increase in the net optical gain can be achieved if the proposed p-doping profile is employed to minimize the effect of nonuniform pumping.

SCIENTIFIC IMPACT OF RESEARCH

Our theoretical and experimental research has contributed substantially to the goal of making 1.3/1.55 micron VCSELs that can meet the most stringent system requirements. Because of the overwhelming advantages of VCSELs over conventional edge emitting lasers in both cost and performance, there is huge market potential for 1.3/1.55 μm VCSELs in data and tele communication and cable TV industries. In addition, there will be applications generated from the unique characteristics of 1.3/1.55 μm VCSELs. These applications include high-speed parallel array interconnect, optical microwave links, phase array antenna, fiber sensors, fiber optic gyroscopes, gas sensing, and medical applications. Because the design concepts and technologies we used to fabricate 1.3/1.55 μm VCSELs are very generic, our work could shed light on the research of mid infrared, visible and UV VCSELs. This is particularly true for InGaSb-based and GaN-based VCSELs.

DEGREES AWARDED

1. Chih-Hsien Jason Lin
   "Design, analysis and fabrication technology for 1.55 micron strained and strain-compensated multiple-quantum-well single frequency lasers," Ph.D., Electrical Engineering, January, 1996

2. Christopher L. Chua
   "Long wavelength vertical cavity surface emitting lasers using wafer-bonded AlAs/GaAs DBR mirrors and strain-compensated multiple quantum well gain media," Ph.D., Electrical Engineering, March, 1996

REFERENCES

[1] J. L. Jewell, A. Scherer, S. L. McCall, Y. H. Lee, S. J. Walker, J. P. Harbinson, and L. T. Florez, "Low threshold electrically-pumped vertical-cavity surface-emitting micro-lasers," Electron. lett., vol. 44, pp. 1123-1124, 1989.

[2] J. A. Lott, R. P. Schneider, Jr., K. J. Malloy, S. P. Kilcoyne, and K. D. Choquette, "Partial top dielectric stack distributed Bragg reflectors for red vertical cavity surface emitting laser arrays," IEEE Photon. Technol. Lett., Vol. 6, no. 12, pp. 1397-1399, 1994.

[3] M. W. Maeda, C. Chang-Hasnain, A. Von Lehmen, H. Izadpanah, Chinlon Lin, M. Z. Iqbal, L. Florez, and J. P. Harbison, "Multigigabit/s operation of 16-wavelength vertical-cavity surface-emitting laser array," IEEE Photon. Technol. Lett., vol. 3, pp. 863-865, 1991.

[4] K. L. Lear, K. D. Choquette, R. P. Schneider, Jr., S. P. Kilcoyne, K. M. Geib, "Vertical-cavity surface-emitting lasers with 50% power conversion efficiency," Technical Digest, Conference on Lasers and Electro-Optics (CLEO), vol. 15, p. 55, 1995.

[5] T. Wipiejewski, D. B. Young, M. G. Peters, B. J. Thibeault, L. A. Coldren, "Etched-pillar vertical-cavity surface-emitting laser diodes with submilliampere threshold currents and high output power," Technical Digest, Conference on Lasers and Electro-Optics (CLEO), vol. 15, p. 55, 1995.

[6] M. H. MacDougal, P. Daniel Dapkus, V. Pudikov, H. Zhao, G. M. Yang, "Use of AlAs oxide/GaAs distributed Bragg reflectors to fabricate ultralow-threshold-current VCSELs," Technical Digest, Conference on Lasers and Electro-Optics (CLEO), vol. 15, p. 56, 1995.

[7] T. Mukaihara, Y. Hayashi, N. Hatori, N. Ohnoki, A. Matsutani, F. Koyama, K. Iga, "0.33-mA threshold InGaAs/GaAs vertical-cavity surface-emitting lasers grown by MOCVD," Technical Digest, Conference on Lasers and Electro-Optics (CLEO), vol. 15, p. 57, 1995.

[8] G. Mong, M. H. MacDougal, and P. Daniel Dapkus, "Ultralow threshold VCSELs fabricated by selective oxidation from all epitaxial structure," CLEO, Postdeadline, CPD4, Baltimore, Maryland, 1995.

[9] W. W. Chow, M. Hagerott Crawford, R. P. Schneider, Jr., "Minimization of threshold current in short wavelength AlGaInP vertical-cavity surface-emitting lasers," IEEE J. Quantum Electronics, vol. 1, pp. 649-653, 1995.

[10] M. Hagerott Crawford, R. P. Schneider, Jr., "Performance of high-efficiency AlGaInP-based red VCSELs," Technical Digest, Conference on Lasers and Electro-Optics (CLEO), vol. 15, p. 168, 1995.

[11] J. J. Dudley, D. I. Babic, R. Mirin, L. Yang, B. I. Miller, R. J. Ram, T. Reynolds, E. L. Hu, and J. E. Bowers, "Low threshold, electrically injected InGaAsP (1.3 micron) vertical cavity lasers on GaAs substrates," Post Deadline, IEEE 51th Device Research Conf., Santa Barbara, CA, June 21-23, 1993.

[12] Y. H. Lo, "Long wavelength vertical cavity surface emitting lasers," LEOS Newsletter, p. 20, Vol. 9, no. 1, 1995.

[13] D. I. Babic, J. J. Dudley, K. Streubel, R. P. Mirin, J. E. Bowers, and E. L. Hu, "Double-fused 1.52 μm vertical-cavity lasers," Appl. Phys. Lett., vol. 66, pp. 1030-1032, 1995.

[14] C. L. Chua, Z. H. Zhu, C. H. Lin, Y. H. Lo, and R. Bhat, "Low threshold 1.57 μm VCSELs using strain-compensated quantum wells and oxide/metal backmirror," IEEE Photon. Technol. Lett., vol. 7(5), pp. 444-446, 1995.

[15] D. I. Babic, K. Streubel, R. P. Mirin, N. M. Margalit, J. E. Bowers, E. L. Hu, Dan E. Mars, L. Yang, K. Carey, "Room-temperature continuous-wave operation of 1.54 mm vertical-cavity lasers," Appl. Phys. Lett., Vol. 67, no. 6, pp. 810-812, 1995.

[16] C. L. Chua, Z. H. Zhu, Y. H. Lo, M. Hong, R. Bhat, ""Long wavelength VCSELs using a wafer-fused GaAs/AlAs Bragg mirror and strain-compensated quantum wells," IEEE LEOS Conference Proceedings, SCL 14.5, p. 420, 1995.

JSEP PUBLICATIONS

1. C. H. Lin, Z. H. Zhu, Y. Qian, Y. H. Lo, Cascaded self-induced holography: a new grating fabrication technology for DFB/DBR lasers and WDM laser arrays," submitted to IEEE J. Quantum Electron., 1996.

2. E. Ejeckam, C. L. Chua, Z. H. Zhu, Y. H. Lo, M. Hong, R. Bhat, "Reliability studies of wafer bonded InGaAs P-I-N photodetectors on Si and GaAs substrates," to be presented in 1996 Conference on Lasers and Electro-Optics (CLEO'96).

3. C.-Y. Tsai, C.-Y. Tsai, R. M. Spencer, Y. H. Lo, and L. F. Eastman, "Nonlinear gain coefficients in semiconductor lasers: Effects of carrier heating," IEEE Journal of Quantum Electronics, vol. 32, no. 2, pp. 201-212, 1996.

4. C. L. Chua, Z. H. Zhu, Y. H. Lo, M. Hong, R. Bhat, "Long wavelength VCSELs using a wafer-fused GaAs/AlAs Bragg mirror and strain-compensated quantum wells," IEEE LEOS Conference Proceedings, SCL 14.5, p. 420, 1995.

5. C. L. Chua, Z. H. Zhu, Y. H. Lo, R. Bhat, M. Hong, "Low-threshold 1.57 micron VC-SEL's using strain-compensated quantum wells and

oxide/metal backmirror," IEEE Photon. Technol. Lett., vol. 7, pp. 444-446, 1995.

6. F. E. Ejeckam, C. L. Chua, Z. H. Zhu, Y. H. Lo, M. Hong, R. Bhat, "High-performance InGaAs photodetectors on Si and GaAs substrates," Applied Physics Letters, vol. 67, no. 26, pp. 3936-3938, 1995.

7. C. Y. Tsai, Y. H. Lo, R. M. Spencer, "Effects of spectral hole burning, carrier heating, and carrier transport on the small signal modulation response of quantum well lasers," Appl. Phys. Lett., vol. 67 (21), pp.3084-3086, 20 November 1995.

8. G. L. Christenson, A. T. T. D. Tran, C. L. Chua, Z. H. Zhu, Y. H. Lo, "WDM transmitters using wavelength tunable vertical cavity lasers and resonant cavity detectors," to be presented in 1996 Conference on *Lasers and Electro-Optics (CLEO'96).*

9. C. Y. Tsai, Y. H. Lo, R. M. Spencer, L. F. Eastman, "Carrier DC and AC capture and escape times in quantum well lasers," IEEE Photonics Technology Letters, Vol. 7, pp. 599-601, 1995.

10. C. Y. Tsai, Y. H. Lo, R. M. Spencer, and C.-Y. Tsai, "Effects of hot phonons on carrier heating in quantum well lasers," IEEE Photonics Technology Letters, vol. 7, no. 9, pp. 950-952, 1995.

11. C. H. Lin, Z. H. Zhu, Y. H. Lo, "New grating fabrication technology for optoelectronic devices: Cascaded self-induced holography," Applied Physics Letters, vol. 67, no. 21, pp. 3072-3074, 1995.

12. C. Y. Tsai, Y. H. Lo, R. M. Spencer, L. F. Eastman, "Nonlinear gain coefficients in semiconductor quantum well lasers: Effects of carrier diffusion, capture, and escape," IEEE J. Selected Topics Quantum Electron., vol. 1, pp. 316-330, 1995.

13. C.-Y. Tsai, Y. H. Lo, L. F. Eastman, "Carrier energy relaxation time in quantum well lasers," IEEE Journal of Quantum Electronics, vol. 31, no. 12, pp. 2148-2158, December 1995.

14. C. H. Lin, Z. H. Zhu, Y. H. Lo, "New technology for fabricating multiple pitch gratings for WDM laser arrays," IEEE LEOS Conference Proceedings, pap. SCL4.1, p. 258, 1995.

15. C. Y. Tsai, Y. H. Lo, R. M. Spencer, L. F. Eastman, C. Y. Tsai, "Degradation of resonant frequency in high-speed quantum well lasers: effects of spectral hole burning, hot carrier, hot phonon, and carrier diffusion-

capture-escape," IEEE LEOS Conference Proceedings, pap. SCL1.4, p. 97, 1995.

16. E. Ejeckam, C. L. Chua, Z. H. Zhu, Y. H. Lo, "High-efficiency Picoamperes Dark Current InGaAs P-I-N Photodetectors on Si and GaAs Substrates," IEEE LEOS Conference Proceedings, pap. IO1.4, p. 23, 1995.

17. C. H. Lin, C. L. Chua, Z. H. Zhu, and Y. H. Lo, "Gratings Fabricated by cascaded, self-Induced holography for DFB Lasers," CLEO Conference Proceedings, p. 339, 1995.

18. C. L. Chua, Z. H. Zhu, Y. H. Lo, R. Bhat, M. Hong, "Long wavelength VCSELs using AlAs/GaAs mirrors and strain-compensated quantum wells," Proceedings of IEEE 15th Biennial Conference on Advanced Concepts in High-Speed Semiconductor Devices and Circuits," pp. 361-363, 1995.

19. C-Y Tsai, Y.H. Lo, R.M. Spencer, L.F. Eastman, C-Yao Tsai, "A Theoretical Investigation for the Effects of Spectral Hole Burning, Hot Carrier, Hot Phonon, and Carrier Diffusion-Capture-Escape on the Limitations of the Modulation Bandwidth in High-Speed Quantum Well Lasers," Proceedings of 15th Biennial Conference on "Advanced Concepts in High Speed Semiconductor Devices and Circuits," pp. 415-424, 1995.

20. C. H. Lin, Z. H. Zhu, Y. H. Lo, "Cascaded self-induced holography: a new fabrication technology for optoelectronics," Proceedings of IEEE 15th Biennial Conference on Advanced Concepts in High-Speed Semiconductor Devices and Circuits," pp.388-397, 1995.

21. F. E. Ejeckam, C. L. Chua, Z. H. Zhu, Y. H. Lo, "High performance InGaAs photodetectors on Si and GaAs substrates," Proceedings of IEEE 15th Biennial Conference on Advanced Concepts in High Speed Semiconductor Devices and Circuits, pp. 194-200, 1995.

HIGH-SPEED DETECTORS WITH INTEGRATED OPTICAL WAVEGUIDE FEEDS

Task #6

Task Principal Investigator: **Richard C. Compton**
Office: (607) 255-9231
Fax: (607) 254-4777
e-mail: rcc7@cornell.edu

OBJECTIVE

The objective of this task is to improve the performance of long-wavelength optical detectors for millimeter-wave applications. In the process this task exploits Cornell's strength in material growth (Shealy) and device simulation (Krusius). Our goal is to optimize the efficiency bandwidth product of detectors with a view to developing devices appropriate for future DoD optoelectronic systems.

We have focused our efforts on the metal-semiconductor-metal (MSM) detector. Its simple material requirements make it relatively easy to integrate with more complex devices such as heterostructure transistors. However, in spite of its simple structure, the MSM photodiode is capable of extremely high speed performance.

The main goals of this task are therefore to develop tools for the design of MSM detectors, establish compatible fabrication process for the integration of HEMTs with detectors, and improve upon the state-of-the-art for measuring these detectors above 50 GHz.

DISCUSSION OF STATE OF THE ART

High speed photodetectors are in demand for lightwave communications, optical computing, sensors, material characterization, and optoelectronic circuits. Photodetectors can be categorized into two groups, photoconductors and photodiodes. In photoconductors, conductivity is increased through the generation of carriers in a semiconductor region located between two ohmic contacts. Photoconductors have been widely used in optoelectronic circuit characterization such as in pump-probe sampling circuits. The response speed of a conventional photoconductor is limited by material properties, namely carrier transit time, carrier lifetime due to recombination, generation, traps, impurities, and carrier diffusion. Recently, photoconductors with response times in the sub-picosecond range have been obtained by material modification processes such as ion implantation to decrease carrier lifetimes[1]. Low-temperature-grown GaAs (LT GaAs) has been also used as substrate material for photoconductive detector with a response time of 1.2 ps

and a bandwidth of 375 Ghz[2]. Because the electrodes of a photoconductor are ohmic, additional charge can be injected at the contacts as a result of differences in hole and electron velocities Noise is a major problem in photoconductors. The finite dark conductivity of the device generates a randomly fluctuating background Johnson noise current.

Unlike photoconductors, photodiodes have a rectifying junction which considerably reduces the Johnson noise when reverse biased. In photodiodes, light absorption and electron-hole pair generation occur in the depletion region. Shot noise generated in the depletion region of photodiodes is considerably smaller than Johnson noise in photoconductors. Quantum efficiency and response speed of photodiodes are closely related parameters. Optimizing response speed by minimizing electrode separation in photodiodes dictates that the active area be small which makes focusing light into the device difficult. Therefore, a compromise has to be made between fast response times and high quantum efficiency.

The fastest compound semiconductor detectors reported are GaAs Schottky barrier photodiodes[3] and metal-semiconductor-metal (MSM) photo-detectors[4,5]. Schottky barrier photodiodes require multi-level fabrication steps with level-to-level alignment for high speed response. In the Schottky photodiode (Fig. 1), incident light passes through a semi-transparent Schottky metal contact and generates electron-hole pairs in the depletion region. The response time is limited either by transit time across the depletion region or the *RC* time constant of the device. To minimize the transit time, a thin absorption layer is desirable but this leads to a large junction capacitance. To reduce the junction capacitance, the active area of the diode should be small. The number of photons collected, however, decreases with smaller area. The minimum active area is ultimately determined by the diameter of the illumination beam. Transparent indium tin oxide (ITO) has been used to serve as an anti-reflection coating and Schottky contact simultaneously, thus reducing the series resistance associated with the thin metal layer and increasing efficiency at the same time[6].

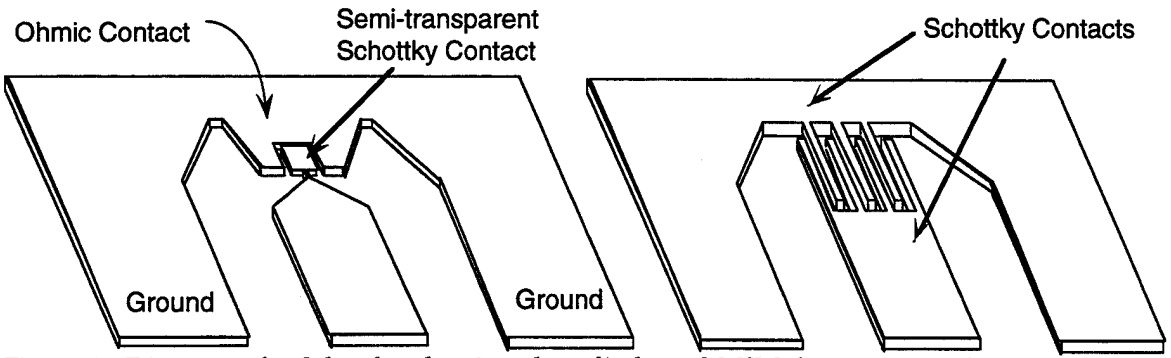

Figure 1. Diagram of a Schottky barrier photodiode and MSM detector in a planar coplanar waveguide configuration. Interdigitated fingers are used in the MSM to produce a large effective cross-section for light incident from the top.

In contrast, the MSM detector (Fig. 1), has a simple, planar horizontal structure, but requires electron beam lithography to achieve the small electrode spacing required for short transit time operation. MSMs have been reported[4] with finger spacings as small as 25 nm and a response time of 0.87 ps on LT GaAs. The low efficiency of MSM photodiodes is due to the shadowing effect of the metal electrodes, reflection at the semiconductor surface and incomplete absorption in the active layer. An anti-reflection coating can be used to reduce the surface reflection. Superlattice structures have been used underneath the absorption layer to enhance the quantum efficiency by reflecting any of the signal which passes completely through the absorbing region back in the device[5].

In an MSM detector, the electrodes form back-to-back Schottky contacts. With an applied voltage, one contact is always reverse biased, and the leakage through this junction (dark current) adversely affects detection sensitivity. Thus dark current is minimized by forming contacts with high Schottky barriers. On GaAs this is readily accomplished. However, with long wavelength (1.3 μm-1.55 μm) detectors using $In_{0.53}Ga_{0.47}As$ absorbing regions a problem arises due to the low barrier heights on this material. High barriers must be obtained by adding a barrier enhancement layer. A number of different materials have been used for this purpose including $In_{0.52}Al_{0.48}As$[7] and InP[8], and more recently strained AlInP[9] and GaInP[10]. The latter obtained very low dark current densities of 4.5 $pA/\mu m^2$.

Another approach to improving the Schottky contact involves passivating the surface states to release the Fermi level pinning, and then using a high work function metal to form the contact. Both phosphidization[11] and sulfide passivation[12] have been tried. With the latter, an MSM detector was fabricated using a sulfur treated InP barrier enhancement layer. The dark currents of this structure were quite high however.

To date, the fastest MSMs operating at the longer wavelengths have been achieved with short lifetime material. Impulse responses approaching 1 ps have been achieved with low-temperature grown GaInAs[13], and an GaInAs/GaAs on GaAs super lattice produced a lifetime-limited response of 3.3 ps[14]. Devices fabricated on long-lifetime material have been reported with responses of 13 ps[15] and 14.7 ps[16], though it should be noted that both these values are possibly influenced by measurement system limitations. The spacing between electrodes for these was 1 μm and 1.4 μm respectively; very little work has been done with sub-micron electrode spacing for long wavelength detectors.

PROGRESS

AlInAs/GaInAs MSM photodetectors have been successfully fabricated on both MOCVD and MBE grown material. These detectors were fabricated with copper Schottky contacts because copper was found to produce a comparable or slightly improved barrier compared to that of Ti/Pt/Au. The devices have very low dark currents, in the low nanoamp regime for biases up to 10 V, and a fast response (17 ps FWHM) which has been characterized by electrooptic sampling. Device operation with intense light and low bias has been investigated and was found to be strongly influenced by the presence of the energy band discontinuities between the GaInAs and the AlInAs.

Also, electrooptic sampling has been used to verify the accuracy of the inductive-loop photoconductive sampling technique developed in the previous reporting period.

i) Copper Schottky Metal: Copper was chosen for the Schottky metal because it was observed that a copper junction appeared to give an improved dark current over that of Ti/Pt/Au. An example of this is seen in Figure 2, where the reverse current density through two large area pads are compared for each type of metallization. The copper current is seen to be half that of the Ti/Pt/Au.

On GaAs the Schottky barrier height depends significantly on the metal type[17]. For example, Au has a barrier height which is 0.13 eV larger than that of Ti for a clean, cleaved surface. This corresponds to a factor of 200 difference in reverse saturation current. It is reasonable to expect that significant improvements in barrier height on AlInAs (or other barrier enhancement materials) may also be achieved by optimization of the metal type. To date no systematic study has been performed on AlInAs to characterize barrier height as a function of metal type. An improved Schottky contact would benefit InP based HEMTs as well as MSM detectors.

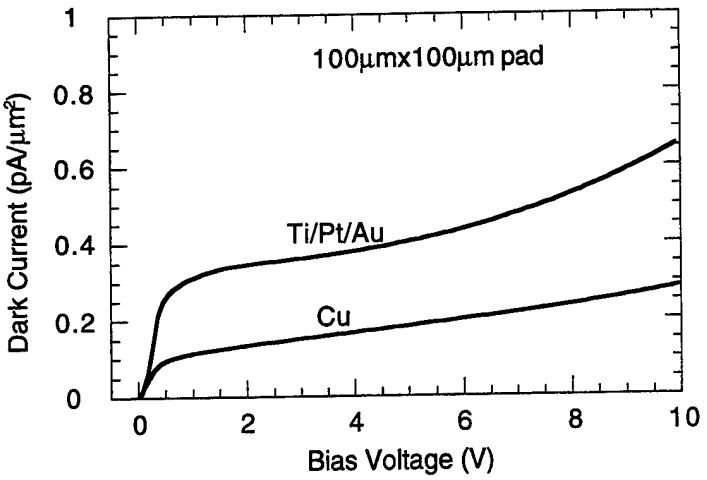

Figure 2. Dark current of large area pads formed with Cu and Ti/Pt/Au metallizations.

Possible drawbacks to using alternate Schottky metals are incompatibility with process steps and junction instability (copper has a very high diffusion coefficient in semiconductors). While evaluating the suitability of copper or other metal contacts for long-life device operation is beyond the scope of this work, it should be noted that a moderate change in device dark current has been observed over a four month period. Figure 3 shows the change, which is a decrease in dark current by roughly a factor of two. This corresponds to an increase in the barrier height of 0.017 eV. Copper contact pads have also been placed in an air oven to determine effects of higher temperatures. Baking at 100 C for 15 minutes decreased the dark current by a factor of 2. An additional 15 minutes at 150 C had no further effect. Increasing the temperature to 250 C caused the dark I-V to change noticeably in shape and the current to decrease further in magnitude. The mechanism causing this behavior has not been investigated.

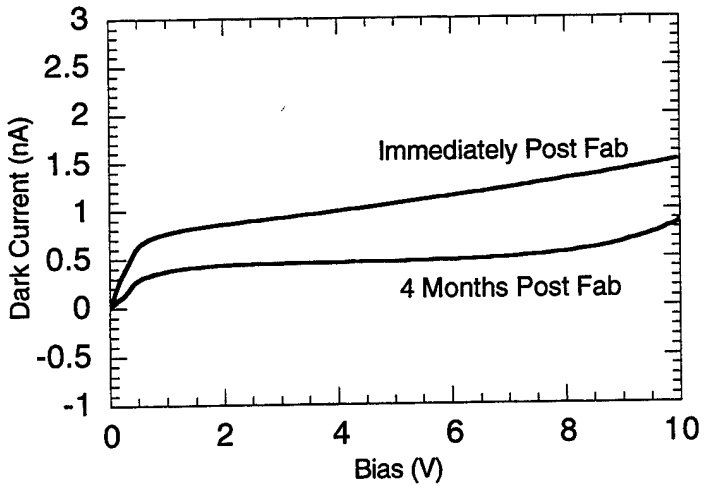

Figure 3. Dark currents obtained immediately after fabrication and four months later for copper Schottky metal.

ii) Device Structure: The material structure used for the devices is as follows: semi-insulating InP substrate, 200 nm InP buffer layer, 900 nm GaInAs absorbing layer, 100 nm AlInAs barrier enhancement layer and a 4 nm layer of GaInAs to minimize oxidation of the aluminum containing layer. (See Figure 4) To remove oxides, processing began with a wet-etch in H_3PO_4/H_2O_2 of approximately 50 nm of AlInAs. Photolithography with image reversal and liftoff was then used to pattern the interdigitated fingers using thermally evaporated Cu (20 nm) and Au (50 nm). Finger width was 1 μm and finger spacing was 1 or 2 μm. Adhesion of the copper to the AlInAs was adequate and caused no processing problems. A wet-etch using a photoresist mask, H_3PO_4/H_2O_2 and HCl/H_3PO_4 (to etch the InP buffer layer) was then made to define a mesa around the active area. Polyimide was spun over the entire substrate and windows were etched using oxygen RIE to allow contact to the Schottky metal. Pads and transmission lines were then formed from 0.5 μm evaporated metal. Some devices were positioned in the ends of 4 mm long coplanar waveguide to permit reflection free sampling of device response.

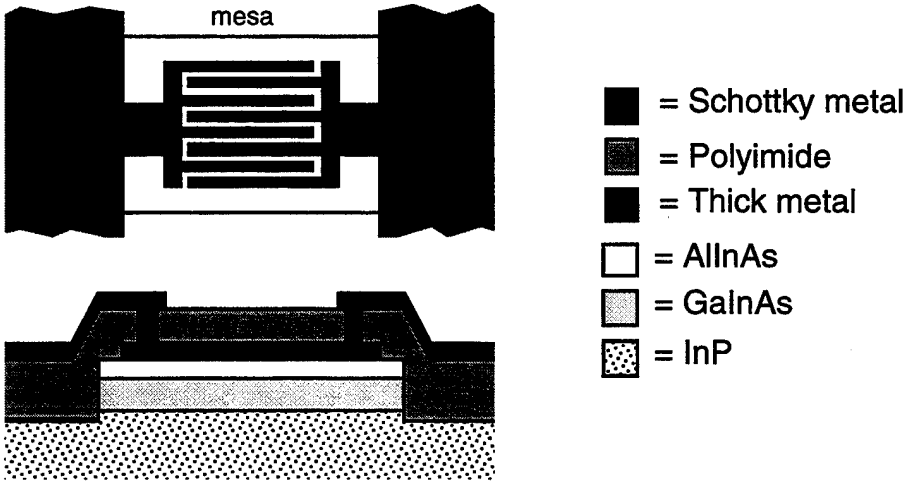

Figure 4. Device structure.

iii) Dark Current: Device dark current is seen in Figure 5 for a device with 2 mm spaces and a 20x20 μm^2 active area. The current at 10 V is 8.3 $pA/\mu m^2$ of annode area, or 3.8 $pA/\mu m^2$ of detection area. This compares very favorably with the best previously reported devices: for a 3 μm spacing device with Ti/Pt/Au on AlInAs[18], the dark current at 10 V was 3 $pA/\mu m^2$ of detection

area; note that smaller dark currents are expected with wider electrode spacing. Current densities obtained with large pads and 30 μm spaces were 0.3 pA/μm^2 at 10 V. The higher dark current of the device compared to the pads is caused by the large perimeter/area ratio of the interdigitated fingers and the narrow finger separation which causes high fields. Based on the thermionic emission theory and a saturation current of 0.1 pA/μm^2 for the large pads, the barrier height is found to be 0.63 eV. This is in reasonable agreement with the value of 6.1 found in[11] for copper on AlInAs.

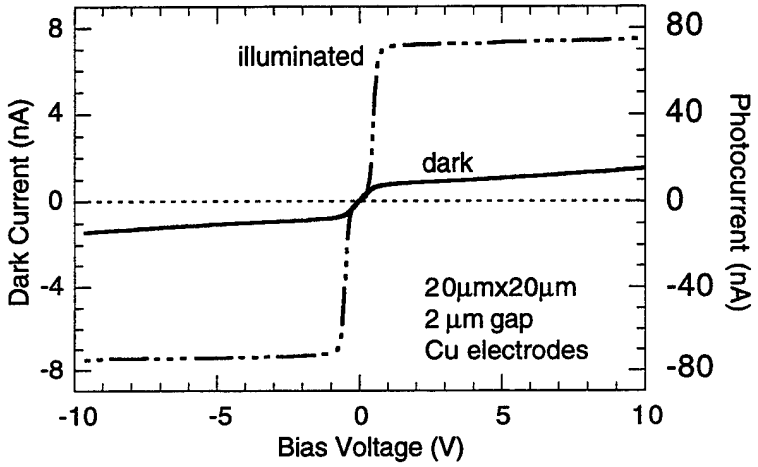

Figure 5. Dark and illuminated currents for a device with 2 μm finger spaces demonstrate symmetric response of back-to-back diodes.

iv) Charge Storage: Photocarriers generated in the absorbing layer must surmount discontinuities in the valence and conduction bands as they pass from the GaInAs into the AlInAs. For the electrons, this barrier is 0.5 eV, and for the holes it is 0.2 eV. At lower biases these discontinuities can cause charge storage at the interface. While it is possible to grade the junction so as to reduce this effect[16], such a device is no longer directly compatible with AlInAs/GaInAs H-MESFET's.

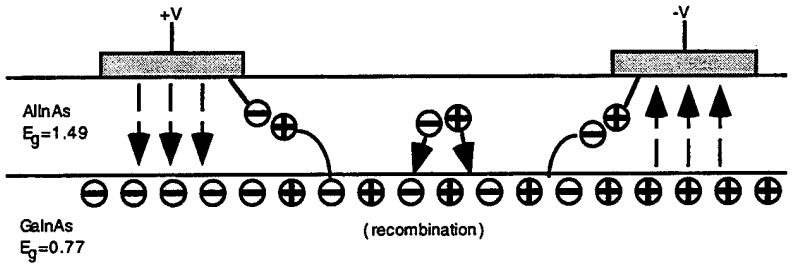

Figure 6. Detector with charge storage. Carriers created far from a contact are trapped in the GaInAs and recombine, and those created close to a contact contribute to the photocurrent.

Charge storage in AlInAs/GaInAs MSM detectors has been studied[18], and the dominant effects are screening of the field in the absorbing region which causes carrier trapping and increased recombination. (Fig. 6) Thus responsivity decreases and transit time for carriers generated in the GaInAs increases. The degree of charge storage depends on both intensity and bias, and is greatest at high intensities and low biases.

In addition to the above, we observed further effects of charge storage. In the limit of extreme charge build-up, the GaInAs becomes conducting and the field is concentrated in the enhancement layer. This results in significant increase of device capacitance due to the thin enhancement layer. This change in capacitance was observed using CW illumination at 633 nm and a network analyzer to measure the complex device impedance at 12.5 GHz. The result is seen in Figure 7, where the capacitance at low bias levels changes by more than a factor of 10 with illumination of 0.4 mW. As bias is increased, greater intensities may be detected before the onset of charge storage.

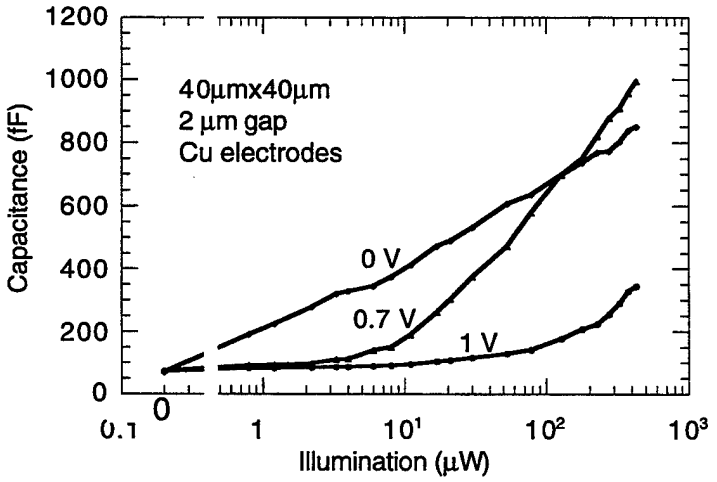

Figure 7. Device capacitance vs. illumination illustrates the effects of charge storage.

A further example of charge storage is found in the temporal response of the devices. Under intense illumination and low bias conditions, devices without an enhancement layer, such as those fabricated on S.I. GaAs earlier in this study, produce a step-like response. The risetime is very fast and the falltime is slow, likely determined by the carrier lifetime. The AlInAs/GaInAs devices, however, exhibit a markedly different behavior. A comparison of the two types of devices is seen in Figure 8, where their responses to an intense 800 nm impulse of light have been measured with a sampling oscilloscope. In contrast to the GaAs device, the AlInAs/GaInAs device produces a small but very fast response (the results in the figure have been normalized - the peak of the AlInAs/GaInAs response is actually about 10 times smaller than the GaAs.) The size of this response scales nearly

linearly with bias; electrical pulses ~0.5 V in magnitude have been attained at biases of 2-3 V. At larger biases, the devices are easily damaged due to the large potential across the thin AlInAs layer. A fast response under similar conditions for a barrier enhanced device has been previously reported[19].

Two mechanisms likely contribute to the fast charge storage response of AlInAs/GaInAs. The first is that screening by charges in the GaInAs layer diminish the field everywhere except in close vicinity to the electrodes. Thus, only carriers generated in the enhancement layer close to the contacts experience a significant field, and only these carriers with short transit times are collected. Secondly, as suggested by [19], the carriers created in the enhancement layer fall quickly into the GaInAs potential so that their lifetime in the AlInAs is short. Both mechanisms rely on carrier generation in the AlInAs so this mode of operation would not be present at longer wavelengths.

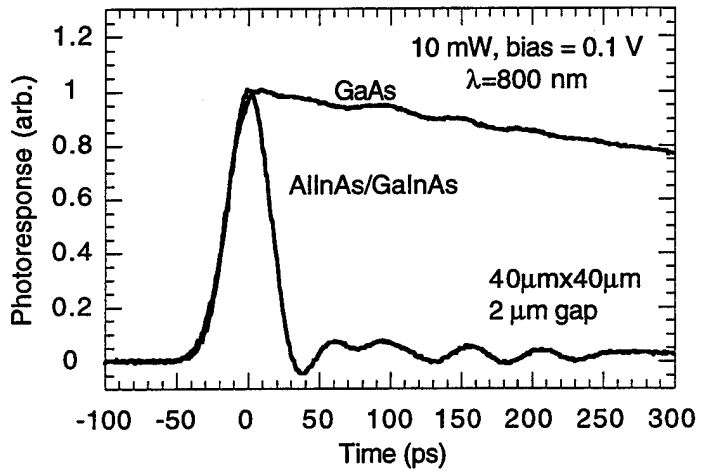

Figure 8. Comparison of AlInAs/GaInAs MSM and GaAs MSM under low bias/ high intensity operation. The fastest response is scope limited.

v) Electrooptic Sampling: The high speed response of the GaAs devices previously fabricated were characterized using photoconductive sampling with an inductive loop[20]. This method relies on the step-like response of the GaAs devices under low bias and high illumination. From the above it is seen that such an approach will not work with the AlInAs/GaInAs devices. Instead, electrooptic sampling with subpicosecond resolution was used to characterize these devices.

The electrooptic sampling system[21,22] used a mode-locked Ti:Sapphire laser at 800 nm and an external $LiTaO_3$ crystal with total internal reflection to sample the signal on the transmission line approximately 800 μm from the device under test. Results for an AlInAs/GaInAs device with 1 μm finger spaces are seen in Figure 9 for a 0.12 pJ optical pulse and a 9 V bias voltage.

Under these conditions charge storage should be minimal. The FWHM is 17 ps and the response is transit time limited. The longer tail is caused mainly by the slower holes, although theoretical studies[23] indicate that even at this bias level there may still be charge storage effects contributing to the long tail. This result is comparable to (2-4 ps slower) the best reported devices to date. The reflection from the end of the bond wire-terminated transmission line is seen at 56 ps.

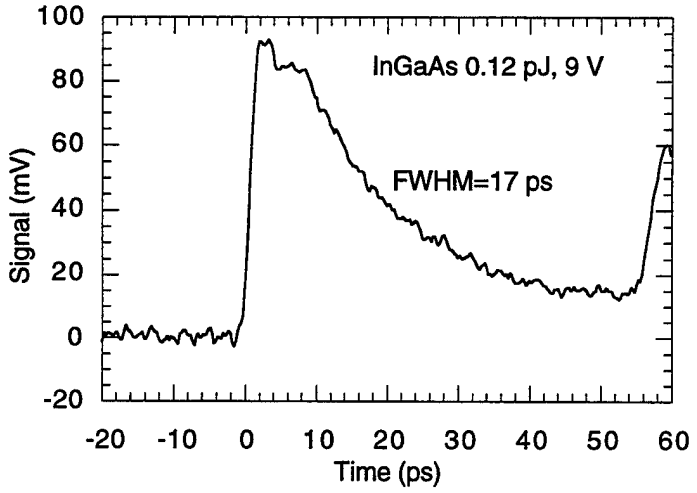

Figure 9. High bias/low intensity response of AlInAs/GaInAs device with 1 μm fingers and spaces. Measured with electrooptic sampling.

The result of sampling the same device in the charge-storage regime of operation is shown in Figure 10. Now, because of the large device capacitance under illumination and the reduced transit time as mentioned above, the response is dominated by the RC time constant. Based on the network analyzer measurements, the capacitance is assumed to be 350 fF for this device; with the 55 ohm transmission line impedance, the decay should have a time constant of 19.3 ps, which is close to the observed value of 20 ps.

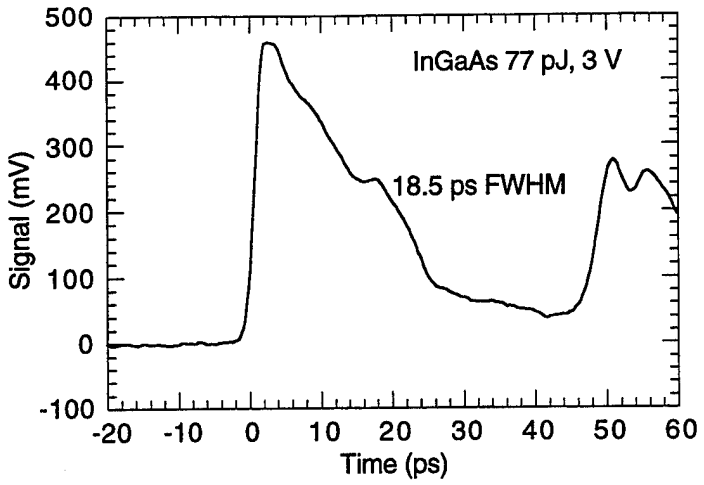

Figure 10. Same device as in Figure 9, operating in the charge storage regime. The decay is now determined by the RC time constant because of the large illuminated device capacitance.

Due to the high-intensity requirements of charge-storage operation (responsivity is reduced for the present devices by more than two orders of magnitude), this mode of operation is not well suited for communications applications. Increasing the enhancement layer thickness to an optimum value should significantly improve both responsivity and speed. Then charge-storage operation may find use in low-bias/high speed detection of sufficiently intense light, or as a means to generate volt-level high-speed electrical transients with a large area planar detector.

vi) Comparison of Inductive Loop and Electrooptic Sampling: The electrooptic sampling result for a GaAs device is seen in Figure 11 and compared with that obtained by inductive loop sampling. It is seen that the agreement between the two methods is quite good. The measurements were made at different voltages, but this should make little difference since the GaAs device response changes little from 5 V to 8 V.

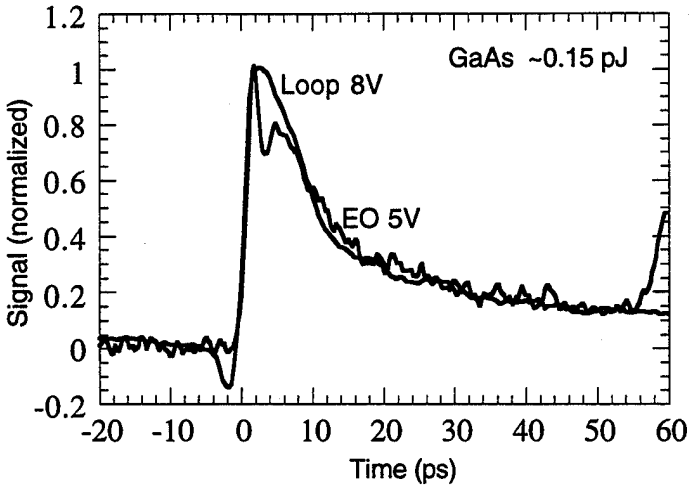

Figure 11. Comparison between sampling with an inductive loop and electrooptic sampling in order to verify the accuracy of the inductive loop method. It is not known what causes the feature near the peak of the electrooptic result.

SCIENTIFIC IMPACT OF RESEARCH

This work highlights the possibility of improving Schottky contacts on AlInAs by proper choice of metal. This has been demonstrated by the fabrication of high performance MSM photodetectors using copper as the Schottky metal. The device performance of 17 ps FWHM and 3.8 pA/μm^2 is comparable to that of the best devices reported for any long-wavelength MSM. Also, device operation with charge-storage has been studied, and identified as a possible low-bias means to detect sufficiently intense high-speed optical pulses and generate volt-level high-speed electrical signals using an MSM detector.

Photoconductive sampling with an inductive loop has been compared to electrooptic sampling and the two methods were found to be in good agreement.

DEGREES AWARDED

None

REFERENCES

[1] F. Doany, D. Grischkowsky, and C. Chi, "Carrier Lifetime vs. Ion Implantation Dose in Silicon-on-Sapphire," *Applied Physics Letters*, 50, 460-462 (1987).

[2] Y. Chen, S. Williamson, T. Brock, F. Smith, and R. Calawa, "375-GHz-Bandwidth Photoconductive Detector," *Applied Physics Letters*, 59 (16), 1984-1986 (1984).

[3] E. Ozbay, K. Li, and D. Bloom, "2.0 ps, 150 GHz GaAs Monolithic Photodiode and All-Electronic Sampler," *IEEE Photonics Technology Letters*, 3, (6), 570-572 (June 1991).

[4] Y. Liu, W. Khalil, P. Fischer, S. Chou, T. Hsiang, S. Alexandrou, and R. Sobolewski, "Nanoscale Ultrafast Metal-Semiconductor-Metal Photodetectors," *50th Annual Device Research Conference Digest*, VIB-1, (1992).

[5] A. Ketterson, J. Seo, M. Tong, K. Nummila, D. Ballegeer, S. Kang, K. Cheng, and I. Adesida, "A 10 GHz Bandwidth Pseudomorphic GaAs-GaInAs-AlGaAs MODFET-Based OEIC Receiver," *ibid*, VIB-5 (1992).

[6] D. Parker, P. Say, and A. Hansom, "110 GHz High Efficiency Photodiodes Fabricated from Indium Tin Oxide/GaAs," *Electronics Letters*, S66-67 (November 1989).

[7] J. Soole, H. Schumacher, H. Leblanc, R. Bhat, and M. Koza, "High Speed Performance of OMCVD Grown InAlAs/GaInAs MSM Photodetectors at 1.5 μm and 1.3 μm Wavelengths," *IEEE Photonics Technology Letters*, 1, (8), 250-252 (August 1989).

[8] C. Shi, D. Grutzmacher, M. Stollenwerk, Q. Wang, and K. Heime, "High-Performance Undoped InP/n-In0.53Ga0.47As MSM Photodetectors Grown by LP-MOVPE", *IEEE Transactions on Electron Devices*, 39, (5), 1028-1031 (1992).

[9] P. T. Chan, H. S. Choy, C. Shu and C. C. Hsu, "High-Performance Metal-Semiconductor-Metal Photodetectors with a Strained $Al_{0.1}In_{0.9}P$ Barrier Enhancement Layer," *Applied Physics Letters*, 67, (12), 1715-1717 (1995).

[10] R. Yuang, H. Shieh, Y. Chien, Y. Chan, J. Chyi, W. Lin and Y. Tu, "High-Performance Large Area InGaAs MSM Photodetectors with a Pseudomorphic InGaP Cap Layer," *IEEE Photonics Technology Letters*, 7, (8), 914-916 (August 1995).

[11] T. Sugino, I. Yamamura, A. Furukawa, K. Matsuda and J. Shirafuji, "Improved Barrier Height of Phosphidized AlInAs," *Sixth IEEEConference on InP and Related Materials*, 632-635 (1994).

[12] I. K. Han, J. Her, Y. T. Byun, S. Lee, D. H. Woo, J. I. Lee, S. H. Kim, K. N. Kang and L. Park, "Low Dark Current and High-Speed Metal-Semiconductor-Metal Photodetector on Sulfur-Treated InP," *Jpn. J. Appl. Phys.*, 33, Pt. 1, No. 12A (1994).

[13] S. Gupta, J. F. Whitaker, S. L. Williamson, G. A. Mourou, L. Lester, K. C. Hwang, P. Ho, J. Mazurowski, and J. M. Ballingall, "High Speed Photodetector Applications of GaAas and $In_xGa_{1-x}As$/GaAs Grown by Low-Temperature Molecular Beam Epitaxy," *Journal of Electronic Materials*, 22, (12), 1449 (1993).

[14] J. Hugi, C. Dupuy, R. Sachot, and M. Ilegems, "Lifetime Limited Ultrafast Response of Metal-Semiconductor-Metal Photodetectors on GaInAs/GaAs-on-GaAs Superlattices," *Electronics Letters*, 29, (12), 1130 (1993).

[15] F. Hieronymi, D. Kuhl, E. H. Bottcher, E. Droge, T. Wolf, and D Bimberg, "High-Performance MSM Photodetectors on Semiinsulating InP:Fe/GaInAs:Fe/InP:Fe," *Fourth International Conference on InP and Related Materials*, 561 (1992).

[16] O. Wada, H. Nobuhara, H. Hamaguchi, T. Mikawa, A. Tackeuchi, and T. Fujii, "Very High Speed GaInAs Metal-Semiconductor-Metal Photodiode Incorporating an AlInAs/GaInAs Graded Superlattice," *Applied Physics Letters*, 54, (1), 16 (1989).

[17] A. B. McLean and R. H. Williams, "Schottky Contacts to Cleaved GaAs (110) Surfaces," *J. Phys. C: Solid State Phys.*, 21, 783-818 (1988).

[18] J. H. Burroughes and M. Hargis, "1.3 mm GaInAs MSM Photodetector with Abrupt GaInAs /AlInAs Interface," *IEEE Photonics Technology Letters*, 3, (6), 532-534 (1991).

[19] S. V. Averin, E. S. von Kamienski, H. G. Roskos, H. J. Geelen, R. Kersting and I. Plettner, "Metal-Semiconductor-Metal Structure with Subpicosecond Resolution," *Tech. Phys.*, 40, (1) 43-47 (1995).

[20] A. C. Davidson, F. W. Wise, and R. C. Compton, "Picosecond Photoconductive Sampling with Nanosecond Carrier Lifetimes Using an Integrated Inductive Loop," *Applied Physics Letters*, 66, (17), 2259-2261 (1995).

[21] S. Alexandrou, R. Sobolewski, and T.Y. Hsiang, "Time Domain Characterization of Bent Coplanar Waveguide," *IEEE J. Quantum Electron.* 28, 2325 (1992).

[22] We acknowledge Marc Currie at the University of Rochester for performing the electrooptic sampling.

[23] E. Sano, "Theoretical Analysis of the Influences of Barrier Enhancement Layers on the Transient Responses of MSM Photodetectors", *IEEE Transactions on Electron Devices*, 39, (6), 1355-1362 (1992).

JSEP PUBLICATIONS

1. A.C. Davidson, F.W. Wise, and R.C. Compton, "Picosecond Photoconductive Sampling with Nanosecond Carrier Lifetimes Using an Integrated Inductive Loop," *Applied Physics Letters*, 66, (17), 2259-2261 (1995).

2. A.C. Davidson, F.W. Wise, and R.C. Compton, "Picosecond Photoconductive Sampling with Nanosecond Carrier Lifetimes Using an Integrated Inductive Loop," in *Ultrafast Electronics and Optoelectronics*, OSA Technical Digest Series, 13 156-158 (1995).

JSEP PRESENTATIONS

1. A.C. Davidson, F.W. Wise, D.T. Emerson, J.R. Shealy and R.C. Compton, "High performance InAlAs/InGaAs MSM Photodetectors with Cu Electrodes," *1996 National Radio Science Meeting*, Boulder CO, Jan. 1996.